

EVALUATING THE HYDROLOGIC RESPONSE TO IRRIGATION
AND AQUIFER STORAGE AND RECOVERY
IN THE REPUBLICAN RIVER BASIN

By
Xiao Liu

A THESIS

Submitted to
Michigan State University
in partial fulfillment of the requirements
for the degree of
Environmental Geosciences—Master of Science

2018

ABSTRACT

EVALUATING THE HYDROLOGIC RESPONSE TO IRRIGATION AND AQUIFER STORAGE AND RECOVERY IN THE REPUBLICAN RIVER BASIN

By

Xiao Liu

Irrigation increases crop production in the US and across the world. The primary source of irrigation in many regions is groundwater pumping, which causes significant water level declines in many agricultural areas. Improved water management strategies that are based on knowledge of the hydrologic responses to irrigation are needed to maintain crop production while moving toward sustainable groundwater irrigation practices. We use an integrated hydrologic model with an embedded irrigation module and newly-developed annual irrigation maps to quantify the recharge, transpiration, streamflow, and groundwater responses to irrigation. Irrigation enhances recharge via return flow across the region, mostly during the growing seasons from June to September.

Aquifer Storage and Recovery (ASR) is a promising water management strategy that may improve water sustainability in intensive agricultural areas. Through ASR, surface water during moderate to high flow conditions could be stored in the adjacent aquifer and recovered for later use. A systematic method was developed to estimate the regional potential for ASR. Potential ASR sites are evaluated in the High Plains Aquifer, according to newly-defined values called natural storage thickness and available water volume. Potential ASR sites are mainly located in the Republican River Basin (RRB) and the central to eastern portions of the Central High Plains.

TABLE OF CONTENTS

| | |
|--|-----------|
| LIST OF TABLES..... | iv |
| LIST OF FIGURES | v |
| INTRODUCTION..... | 1 |
| CHAPTER 1 HYDROLOGIC RESPONSE TO IRRIGATION..... | 5 |
| 1.1 INTRODUCTION..... | 5 |
| 1.2 METHODS | 7 |
| 1.2.1 Site Description and Data | 7 |
| 1.2.2 Simulating Integrated Surface and Subsurface Hydrology | 10 |
| 1.2.3 Time-Varying Irrigation Area and Behavior | 17 |
| 1.3 RESULTS AND DISCUSSIONS..... | 19 |
| 1.3.1 Calibration of Annual Irrigation Thresholds..... | 19 |
| 1.3.2 Hydrologic Changes due to Irrigation | 23 |
| 1.3.3 Efficient Irrigation Range..... | 25 |
| 1.3.4 Irrigation Performance and Sustainability | 28 |
| 1.4 CONCLUSIONS | 32 |
| REFERENCES..... | 35 |
| CHAPTER 2 POTENTIAL OF AQUIFER STORAGE AND RECOVERY | 41 |
| 2.1 INTRODUCTION..... | 41 |
| 2.2 METHODS | 45 |
| 2.2.1 Water Availability of Potential ASR Sites | 46 |
| 2.2.2 Criteria for Potential ASR Sites | 48 |
| 2.3 RESULTS AND DISCUSSIONS..... | 51 |
| 2.3.1 Potential ASR Sites across the HPA | 51 |
| 2.3.2 Potential ASR Sites in the Republican River Basin (RRB) | 52 |
| 2.3 CONCLUSIONS | 58 |
| REFERENCES..... | 60 |

LIST OF TABLES

| | |
|--|----|
| Table 1.1 Zonal kriging models, parameters and predictions errors for K and S_y . <i>Semivariogram is used except where covariance is given, which means covariance variogram is used.</i> | 15 |
| Table 1.2 Model calibration. | 16 |
| Table 1.3 The adjustment factor of plant available water fraction for simulated irrigation. | 21 |
| Table 2.1 Average storage area in the Western portion of the Republican River Basin (km^2). | 55 |

LIST OF FIGURES

| | |
|---|----|
| Figure 0.1: Study area. <i>Irrigation area is the 2012 MODIS data from Pervez and Brown (2010).</i> | 2 |
| Figure 0.2: Diagram of the theoretical framework. | 3 |
| Figure 1.1: Model input data: (a) land use, (b) numbers of years irrigated (<i>modified from Deines et al., 2017</i>), and (c) precipitation across the domain. <i>Blue circles represent selected wet years; black open circles are selected normal years; red circles represent selected dry years.</i> | 8 |
| Figure 1.2: Model framework diagram. | 11 |
| Figure 1.3: Maps of key model parameters. (a-b) Hydraulic conductivity of model layers (<i>high K is set for reservoirs</i>), layer 1 has separate interpolated K values for alluvial areas, (c) Specific yield of the first model layer (S_y of the second layer not shown here has only non-alluvial zone interpolated), and (d) groundwater model boundary conditions. <i>Hydraulic conductivity and specific yield values were interpolated from point data using zonal (alluvial and non-alluvial zones) kriging. Stream and drain cells were simulated using the SFR2 and drain packages of MODFLOW, respectively.</i> | 14 |
| Figure 1.4: Simulated versus observed (a) water levels, (b) water levels residuals, and (c) streamflows. | 16 |
| Figure 1.5: Diagram of the irrigation module framework. | 19 |
| Figure 1.6: Simulated versus observed regional irrigation. (a) Domain averaged irrigation, (b) calibrated irrigation parameters, (c) down-scaled observed 15-year-average (2002-2016) irrigation map, and (d) simulated 15-year-average (2002-2016) irrigation map. | 22 |
| Figure 1.7: Maps of 15-year-average (2002-2016) simulated changes in: (a) return flow, (b) overland runoff, (c) return flow to recharge ratio, and (d) evapotranspiration due to estimated actual irrigation. | 24 |
| Figure 1.8: Simulated actual hydrologic change to actual irrigation across the domain. (a) Estimated monthly return flow, (b) increased percentage recharge with irrigation, and (c) increased overland runoff with irrigation. <i>Grey areas indicate the growing season (120-235th day of the year).</i> | 25 |
| Figure 1.9: Hydrologic changes with different irrigation water. (a-b) Domain-average net recharge and overland runoff changes with irrigation, and (c-e) irrigated-land-average overland runoff, net recharge, and ET changes during the growing season to irrigation. (d) Recharge is the vertical | |

distance between the colored lines and the grey 1:1 line; *the recharge of nearly zero irrigation (the first point) is proximate to natural recharge; return flow is the difference between recharge and the natural recharge.*..... 28

Figure 1.10: Reduced versus observed (a) irrigation water applied in the model, (b) water balance across the domain, and (c) accumulated net recharge across the domain. *Pumping water is the amount required for groundwater-based irrigation based on the observed annual pumping ratio.* 30

Figure 1.11: Domain-averaged water level changes based on 2003. 32

Figure 1.12: Maps of water level changes between 2016 and 2003. (a) Observed changes, (b) baseline, (c) reduced, and (d) simulated differences between reduced and baseline scenarios. 32

Figure 2.1: Conceptual diagram of flow (a) interpolation, and (b) extrapolation. *The most upstream point of a stream from the flow accumulation grid is assigned zero flow.* 47

Figure 2.2: Hydraulic gradient map of the High Plains Aquifer in 2015. *(Calculated based on 2015 water table elevation maps from Haacker, et al 2016).* 50

Figure 2.3: Conceptual diagram of the ASR natural storage zone. 50

Figure 2.4: Estimated ASR potential in the High Plains Aquifer includes analysis of: (a) current natural storage thickness *(Calculated based on 2015 water table elevation maps from Haacker, et al 2016)*, and (b) average available water volumes for potential ASR sites from 1997 to 2016. *Natural storage is not shown where transmissivity < 93m²/d and saturated thickness < 8 m, because these areas likely do not have sufficient potential for ASR due to ineffective storage and recovery. Most areas with saturated thickness < 8 m also have transmissivity < 93m²/d, thus the overlapped area is not shown in the figure. Available water is defined as the streamflow minus the in-stream use; the Republican River Compact regulations are used later relative to the total streamflow at the NE-KS border.* 52

Figure 2.5: Potential ASR sites in the Republican River Basin can be identified by evaluating (a) natural storage thickness, (b) storage water depth, and (c) available water. *Storage water depth is defined as the product of natural storage and specific yield.* 54

Figure 2.6: Map of potential ASR sites in the upper Republican River basin showing (a) natural storage thickness, (b) storage water depth, and (c) sites map. *A 5 km-stream-buffer is shown between dashed lines as ASR is generally cost-effective with short transport distances. The points labeled “Large ASR water source” are USGS gauges that could offer similar water source as the Equus Bed ASR project. The predevelopment water table of most gaining river areas would have been near the land surface.* 56

Figure 2.7: Observed mean monthly discharge at USGS gaging stations near potential ASR sites in the upstream portions of the Republican River basin. *Growing months were defined as May-August. (a), (b), and (c) refer to three gauges with station numbers 06835500, 06837000, and 06843500. They are also labeled “Large ASR water source”(green solid circles) from left to right in Figure 2.6.*..... 57

Figure 2.8: 20-year-average (1997-2016) monthly mean flow at USGS gaging stations near potential ASR sites in the upstream portions of the Republican River basin. *MDS refers to the inferred Minimum Desirable Streamflow. (a), (b), and (c) refer to three gauges with station numbers 06835500, 06837000, and 06843500.*..... 58

INTRODUCTION

The High Plains Aquifer, with saturated thicknesses from 15 to over 300 m, underlies more than 450,000 km² of 8 states, including South Dakota, Wyoming, Nebraska, Colorado, Kansas, Oklahoma, Texas, and New Mexico (USGS 2011). Before large scale development of groundwater from the aquifer, it stored more than 3,900 km³ of water (Haacker et al. 2016; McGuire 2009). Due to groundwater pumping to irrigate croplands, the aquifer storage had declined by approximately 406 km³, which is more than 10% of the total storage (Haacker et al. 2016). Average annual total aquifer recharge for the HPA has been estimated between 4.5 and 14 km³, compared to average annual irrigation withdrawals of 30 km³ (McGuire 2009).

The Republican River Basin (RRB) covers about 65,000 km² of the Northern HPA. Due to its central location on the continent along the leeward side of the Rocky Mountains, annual rainfall ranges from less than 40 cm in the west to more than 60 cm in the eastern portion of the basin (NLDAS). According to the Great Plains Hydrologic Observatory in the RRB, from its headwater drainage to the Nebraska-Kansas state line, the mean annual runoff to area ratio ranges from less than 0.5 cm in the western area of the basin to about 7 cm at the eastern end (Great Plains WATERS Network Observatory 2014). Due to large-scale groundwater development, streamflow has decreased dramatically. Kansas sued Nebraska in 1999 for violating the Republican River Compact of 1942, which allocated each state a portion of the fixed basin water supply (Peck 2007). By 2004, in accordance with the compact by the US Supreme Court, measures were implemented to restrict groundwater use and maintain the transboundary streamflow from Nebraska into Kansas.

Changes in irrigation to meet streamflow targets can directly affect future crop production and local climate, which influence peoples' livelihoods across the RRB. We explore the hydrologic response to irrigation to evaluate the efficiency of irrigation performance and the effects of irrigation practices on streamflows in the Republican River Basin. Aquifer Storage and Recovery (ASR), is one management strategy that could decrease the negative effects of irrigation across the region. We evaluated the potential viability of aquifer storage and recovery practices across the HPA, including how it could potentially be used to meet required in-stream flows while providing sufficient water for irrigation.

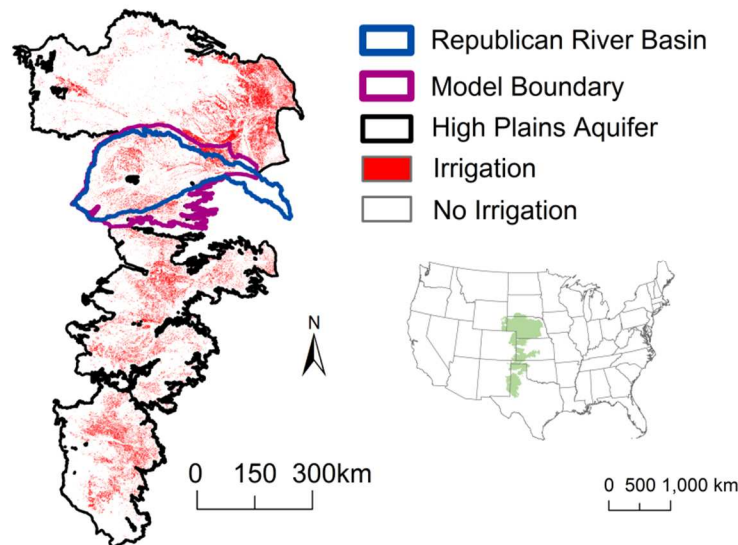


Figure 0.1: Study area. *Irrigation area is the 2012 MODIS data from Pervez and Brown (2010).*

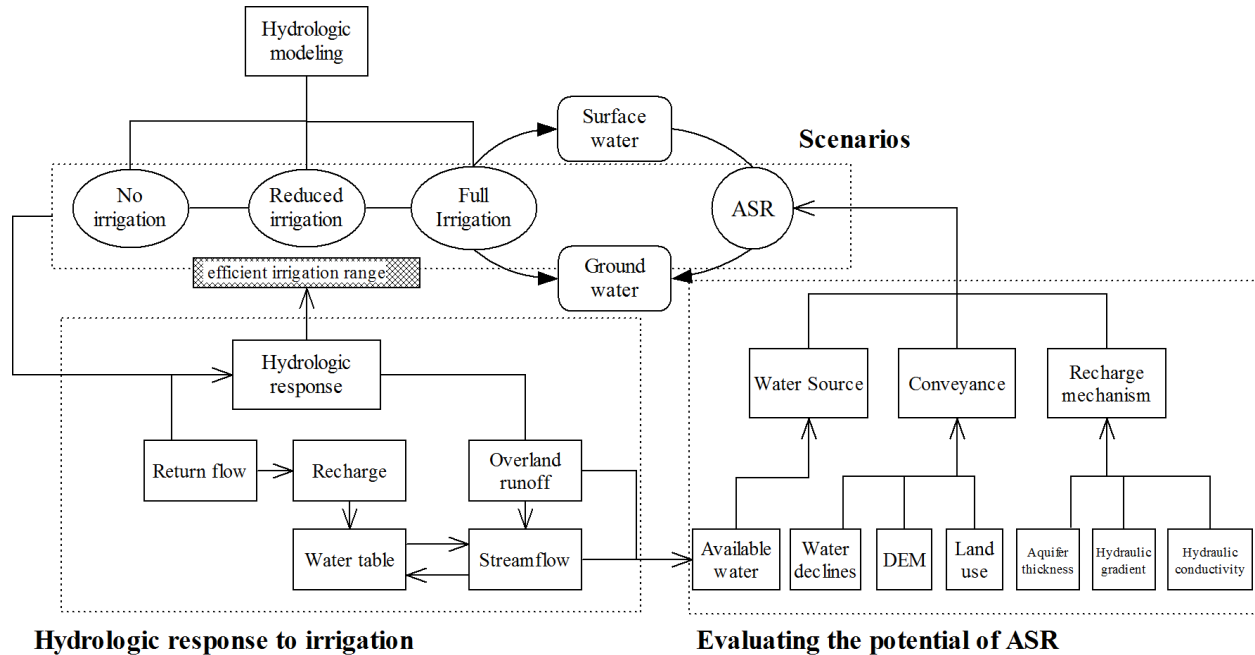


Figure 0.2: Diagram of the theoretical framework.

The central idea of water use and management is water relocation. Although irrigation using a surface water source can enhance groundwater recharge, most irrigation across the High Plains Aquifer uses groundwater as its source. ASR is an effective water management strategy for some regions, which relocates surface water back to groundwater. Therefore, several questions this research attempts to answer are:

Question 1: How have changing irrigation practices across the RRB affected the hydrology of the region?

Question 2: What level of reductions in irrigation across the RRB would likely be sustainable?

This research addresses these two questions by quantifying hydrologic response to irrigation via modeling multiple irrigation scenarios. By modeling irrigation and non-irrigation scenarios, hydrologic responses to irrigation could be quantified in terms of return flow, recharge, overland runoff, groundwater levels, and streamflow. We estimate an efficient irrigation range within which

irrigation meets crop water requirements without significant enhancement of runoff. The Kansas Local Enhanced Management Areas (LEMAs) recently reduced irrigation by ~20 % of the average irrigation from 2002 to 2016. The water balance of reduced irrigation scenario is examined in terms of potential sustainability.

Question 3: What regions might be promising for ASR to potentially relieve the water table declines across the High Plains Aquifer?

Question 4: For the Republican River Basin, how much impounded water could be stored via ASR?

We address these two questions by evaluating ASR scenarios that include a range of water sources, conveyances, and recharge mechanisms. Water source involves where and how much water is available; conveyance involves how water can be delivered to areas where it is needed; and recharge mechanisms reveal where impounded water can be efficiently stored and retrieved. The advantages and disadvantages of a range of techniques are summarized to help identify mechanisms that will best enhance recharge.

CHAPTER 1 HYDROLOGIC RESPONSE TO IRRIGATION

1.1 INTRODUCTION

A large proportion of crop production is supported by irrigation globally. In the United States, about 55.8 million acres of cropland were irrigated in 2012 (USDA 2012), with ~39% this using groundwater as a source on average from 1985 to 2010 (USGS water use data from NWIS). Groundwater pumping for irrigation causes significant water level declines in many agricultural areas (e.g., Whittemore et al. 2016; Konikow 2013). Increasing water declines are decreasing saturated thickness to the point where many areas are no longer able to irrigate. Quantifying the hydrologic responses to irrigation could provide a basis to design efficient irrigation and other water management strategies.

Numerous studies have simulated the hydrologic effects of irrigation. These include demonstrations of evapotranspiration enhancement and temperature reductions at a large scale by hydro-meteorological models (Lobell and Bonfils 2008; Ozdogan et al. 2010; Pei et al. 2016), and groundwater and streamflow consumption (Pokhrel et al. 2015; Zeng and Cai 2014). For example, a large scale hydrologic model simulation shows surface irrigation leads to decreased streamflow and increased evapotranspiration in the Colorado and Mekong River Basins (Haddeland and Lettenmaier et al. 2006). Ground water irrigation resulted in a significant water storage decline in the two large irrigated aquifers (the High Plains Aquifer and Central Valley aquifer) of the US (Pokhrel et al. 2015). In addition of increased evapotranspiration, reduced surface sensible heat flux by irrigation is found over irrigated areas of the US during the growing season (Ozdogan et al. 2010). Also large scale irrigation's effects on precipitation have been quantified across the United

States by Pei et al. (2016).

Most publications (Boucher et al. 2004; Lobell et al. 2006; Kueppers et al. 2007) have either focused on changes of regional climate or have only accounted for limited hydrologic processes. There are few studies that have accounted for the full water and energy balance with a high resolution model across large aquifers. Here, we explore the influence of irrigation across the Republican River Basin (RRB), which is a portion of the High Plains Aquifer, on groundwater recharge, return flow, streamflow, and groundwater levels using an integrated hydrology model. Analysis of the hydrologic response to irrigation could provide a basis for improved water management, including how to efficiently apply irrigation and design resource enhancement projects, such as Aquifer Storage and Recovery (ASR). Such efforts could increase water productivity and enhance the associated economic and environmental benefits. Quantifying water balance components associated with irrigation changes are important to evaluate irrigation performance (Taghvaeian and Neale 2011). Efficient irrigation strategies can be developed for regions such as the RRB by simulating the hydrologic response to a range of potential irrigation scenarios. Prior research on irrigation performance generally focused on surface water source irrigation in a scale of one or several irrigation districts including evaluation of evapotranspiration, crop yields, and water productivity (crop yield per unit water use) either via the data (Ahmad et al. 2009) or irrigation simulations (Jiang et al. 2015).

Here, we compare simulated versus observed irrigation rates across time and space for a groundwater source across the RRB by accounting for the full energy and water balance. We also estimate an efficient irrigation range within which irrigation meets crop water requirements

without significant runoff enhancement. Finally we discuss the irrigation performance and sustainability for these irrigation scenarios.

1.2 METHODS

1.2.1 Site Description and Data

The Republican River Basin (RRB) spans 65,000 km² across Nebraska, Colorado, and Kansas over the Northern High Plains Aquifer. The RRB land use is predominantly agricultural and grassland (Figure 1.1a), with a long history of irrigation. Our analysis uses high resolution maps of annual irrigation developed using LANDSAT (Deines et al. 2017); the total number of years irrigated from 1999 to 2016 is shown in Figure 1.1b. The climate for the basin ranges from semi-arid in the west to sub-humid in the east with precipitation from 300 to 600 mm annually, over half of which falls during the growing season (Figure 1.1c).

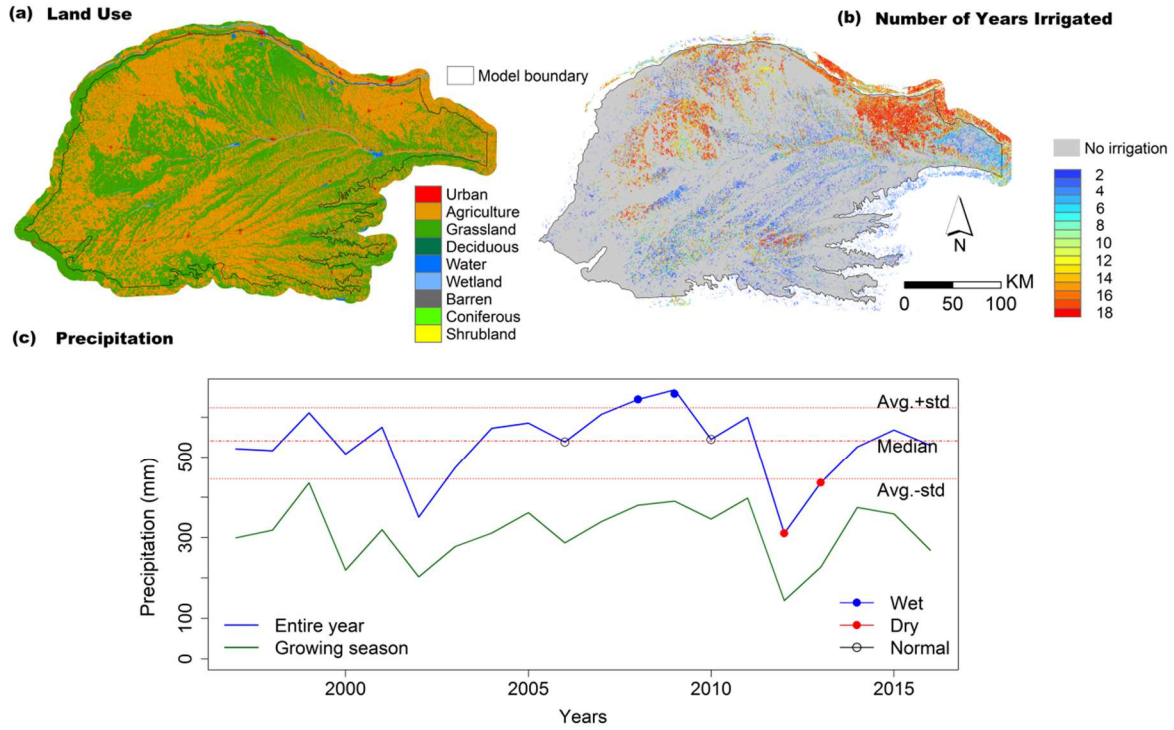


Figure 1.1: Model input data: (a) land use, (b) numbers of years irrigated (*modified from Deines et al., 2017*), and (c) precipitation across the domain. *Blue circles represent selected wet years; black open circles are selected normal years; red circles represent selected dry years.*

Input data for our model are from readily-available public GIS, remote-sensing, and modeling sources. Climate data, including precipitation, temperature, wind speed, solar radiation, specific humidity were extracted from the North American Land Data Assimilation System 2-a forcing dataset (NLDAS-2). Soil textural properties were derived from standardizing layers and weighting across components within the USDA's Soil Survey Geographic (SSURGO Soil Survey Staff). Soil hydraulic properties were derived from these textures and the ROSETTA database (Schaap and Leij et al. 2001). Hydrographic data are from the 1:24,000-scale National Hydrography Dataset (NHD). Wetlands are classified and located using the National Wetlands Inventory (U.S. Fish and Wildlife Service 2014). Land use at 30 meter spatial resolution was extracted from the National

Land Cover database 2011 (NLCD 2011), created by the Multi-Resolution Land Characteristics (MRLC) Consortium (Homer et al 2015). Topographic information is derived from the US National Elevations Dataset (NED) 1" DEM. Leaf Area Index (LAI) data before 2003 is from the MODIS 15 LAI/FPAR 8-day product, which characterizes spatial and temporal variations at approximately 1 km resolution (Myneni et al. 2015). LAI data from 2003 to 2016 is given by the MODIS 15 LAI/FPAR 4-day product with 500 meter pixels (Myneni et al. 2015). Aquifer hydraulic conductivity and specific yield values were interpolated using zonal (alluvial and other zones) kriging based on point data from wells drilled into the Northern High Plains Aquifer. This point data (Houton and others 2013) was obtained using the Geoparm macro and automatically assigning K and S_y to the lithology represented at a given well on the basis of drill cutting description of the lithology from logs.

Observation data was used for model validation and calibration. Irrigation water use records are not publicly available for most portions of this region except Kansas at the level of individual wells. However, the Republican River Compact Administration (RRCA) derived annual county-level pumping estimates by combining pumping records and total irrigated acres by source (surface water and groundwater). They then weighted the annual county pumping estimates by the amount of sprinkler and flood irrigation, and then distributed it to cells at 1 mile resolution by the weight of the well capacity for irrigation wells (RRCA 2003). Water level measurements including well location, altitude and depth to groundwater were obtained from the United States Geological Survey (USGS). These groundwater level data were also combined with static water levels from wells listed as points of diversion from the Nebraska Department of Natural Resources (DNR) for

model calibration. The 250 m interpolated water table maps from Haacker et al., (2016) were also used as the observed water levels for comparison (Haacker et al., 2016). Daily discharge for gauges was gathered from the USGS National Water Information System (NWIS).

1.2.2 Simulating Integrated Surface and Subsurface Hydrology

Integrated surface and subsurface hydrology was simulated using the Landscape Hydrology Model (LHM), which is a process-based, fully distributed hydrologic model, capable of high-resolution modeling at regional scales (Hyndman et al. 2007; Kendall 2009; Wiley et al. 2010; Luszcz et al. 2017). LHM simulates the entire terrestrial hydrologic cycle with process-based component modules interacting with hourly timesteps. These modules are: canopy hydrology, depression storage, soil moisture, temperature, snowpack, ET, wetland hydrology, irrigation, and runoff. LHM uses MODFLOW, the U.S. Geological Survey's modular finite-difference groundwater flow code (Harbaugh et al 2000, 2017) to simulate saturated groundwater flow. The runoff module routes overland flow from externally-drained upland and wetland cells to channels, and internally-drained runoff to storage within basin sinks. Here, the LHM runoff module is coupled with the SFR2 package of MODFLOW to simulate streamflow, which interacts with groundwater.

For the root zone (extending from the surface down to approximately 2.5 meters), LHM calculates each term in the water balance equation (Hyndman et al. 2007; Kendall, 2009):

$$\Delta S = P - T - E - P_c + T_r - E_x - R$$

Where, ΔS is the change of soil moisture storage, P is watershed available precipitation, T is transpiration, E is evaporation, P_c is deep percolation beneath the biologically active soil zone, T_r

is lateral near-surface unsaturated flow, and E_x is the exfiltration from each cell, and R is precipitation excess runoff. Deep percolation is then routed through a 1-D unsaturated zone module that generates groundwater recharge by delaying the deep percolation pulses. MODFLOW then solves the groundwater flow equation, calculates water levels and boundary condition fluxes.

LHM has multiple inputs including climate, soil, wetland, topography, LAI, and land use data. It simulates irrigation water applied, recharge, ET, overland runoff and groundwater levels, streamflow and groundwater ET (Figure 1.2).

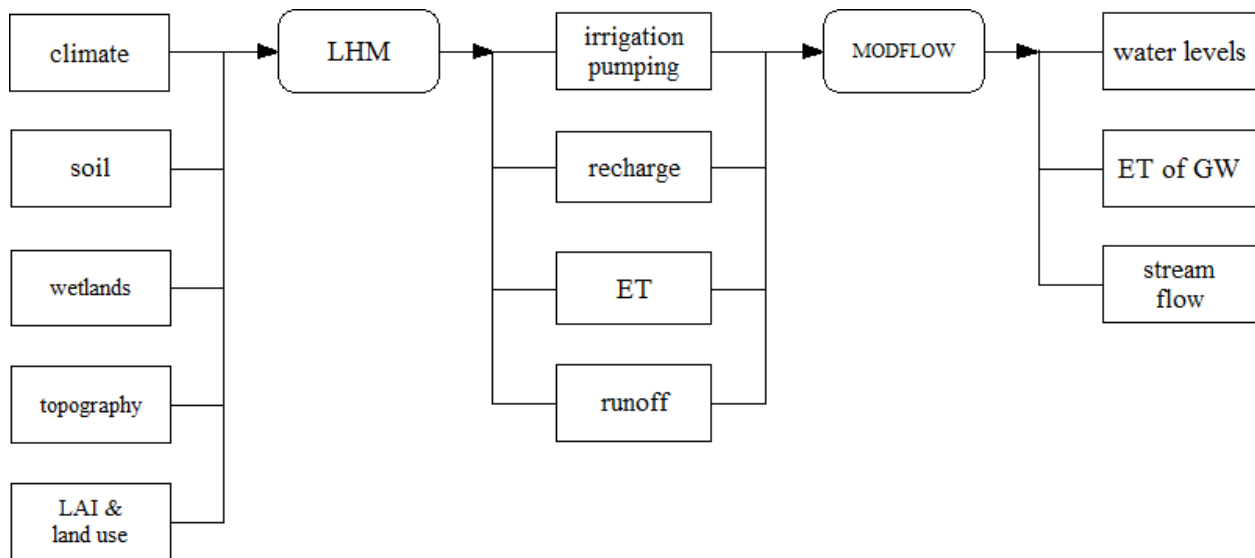


Figure 1.2: Model framework diagram.

A LHM model of the RRB was run with hourly time steps and 600 m cells. Recharge and phreatic ET-demand fluxes were fed into a two layer groundwater model with monthly stress periods. The groundwater model (Figure 1.3d) was built in MODFLOW with drain, ET, and SFR2 packages. Groundwater layer elevations were determined by dividing the saturated thickness of the aquifer into two layers with approximately equal thickness. Aquifer base elevations were interpolated from the 200 m interval aquifer base contour map (Cederstrand et al. 1998). Starting

heads for the model were taken from the interpolated 1997 map of water table elevations (Haacker et al. 2016). Hydraulic conductivity values (Figures 1.3a, b) and specific yield (Figure 1.3c) were derived by kriging well data from alluvial and non-alluvial zones separately. Well data within a 2 km buffer of streams were selected for the alluvial zone while others were included for non-alluvial zone estimates. Multiple semivariogram models with 1000 to 4500 lag sizes were evaluated; other parameters are automatically estimated by Geostatistical Analyst tool in Arc-GIS with nugget set true; the selected model had the lowest mean standardized and root-mean-square standardized errors (Table 1.1).

We divided the 1997 to 2016 modeling period into model spin-up and simulation periods. Since LAI and high resolution observed irrigation data were not available from 1997 to 1999, for this period we tested two pseudo irrigation scenarios: (1) with no irrigation, and (2) with irrigation from 2000. Simulated water level changes from 2003 to 2016 were similar for these two scenarios, thus 1997-2002 was considered as spin-up period, and 2003-2016 as simulation period. Since LAI from 2000 has been used for 1997-1999, we adopted the second pseudo irrigation scenario to keep data consistency.

The LHM runoff module provided overland flow estimates to the SFR2 package, including the routed external runoff over uplands and wetlands, stream evapotranspiration, and stream width. Stream depth was estimated using Manning's equation in the SFR2 package, with an assumed wide rectangular channel for simplification (Niswonger et al. 2005). In Manning's equation, streamflow is a function of stream depth and other parameters including roughness. In the stream water balance equation, streamflow is a function of components from multiple sources including

stream leakage, which is a function of stream depth. Thus by the combination of these two equations, stream depth will be estimated to calculate the streamflow and stream leakage. The Manning's roughness coefficient was set to 0.035 across the domain, which is a typical value for natural channels (Chow 1959). Vertical hydraulic conductivity of the streambed was assumed equal to the kriged alluvial horizontal hydraulic conductivities, and streambed elevation was set at the surface elevation of stream cells from the DEM. Flow from overland runoff is routed down the channels (through 264 stream segments) and simultaneously interacts with groundwater (Figure 1.3d). Based on the RRCA observed surface irrigation map, 69 segments along the mainstem used surface irrigation; the irrigation amount for each segment was divided by the product of segment length and width to get an irrigation depth, which was then removed during the growing season.

Depression storage is a key parameter that affects interactions between irrigation and hydrology. Farmers manage this component of the landscape to enhance water retention on their fields. For instance, ridge-tilling involves planting seeds in the valleys between carefully molded soil ridges, which can be aligned along topographic contours, increases depression storage that can be further enhanced using crop residues (MDA 2011; Garg et al 2017). Total depression storage capacity used in LHM was determined by land use, soil texture, and slope class from a tabular reference of storage capacities (Manfreda et al. 2005); this reference provided initial depression storage capacity in agricultural lands between 0.23 and 3 mm across a variety of soil textures, slopes and tillage methods. Field experiments have shown depression storage initially ranges from 15 to 35 mm and later drops to 4-8 mm with accumulated rain in tilled fields (Guzha 2004). Thus the tilled fields have storage capacity 2-25 times larger than non-tilled fields even with

accumulated rain. According to USDA census data (USDA 2012), 79% of agricultural lands in Nebraska are tilled. Considering this 79% ratio and average nearly 13 times larger storage capacity in tilled field, we use the depression storage capacity from Manfreda et al. (2005) multiplied by 10 to provide a better match to the field experiments under tillage.

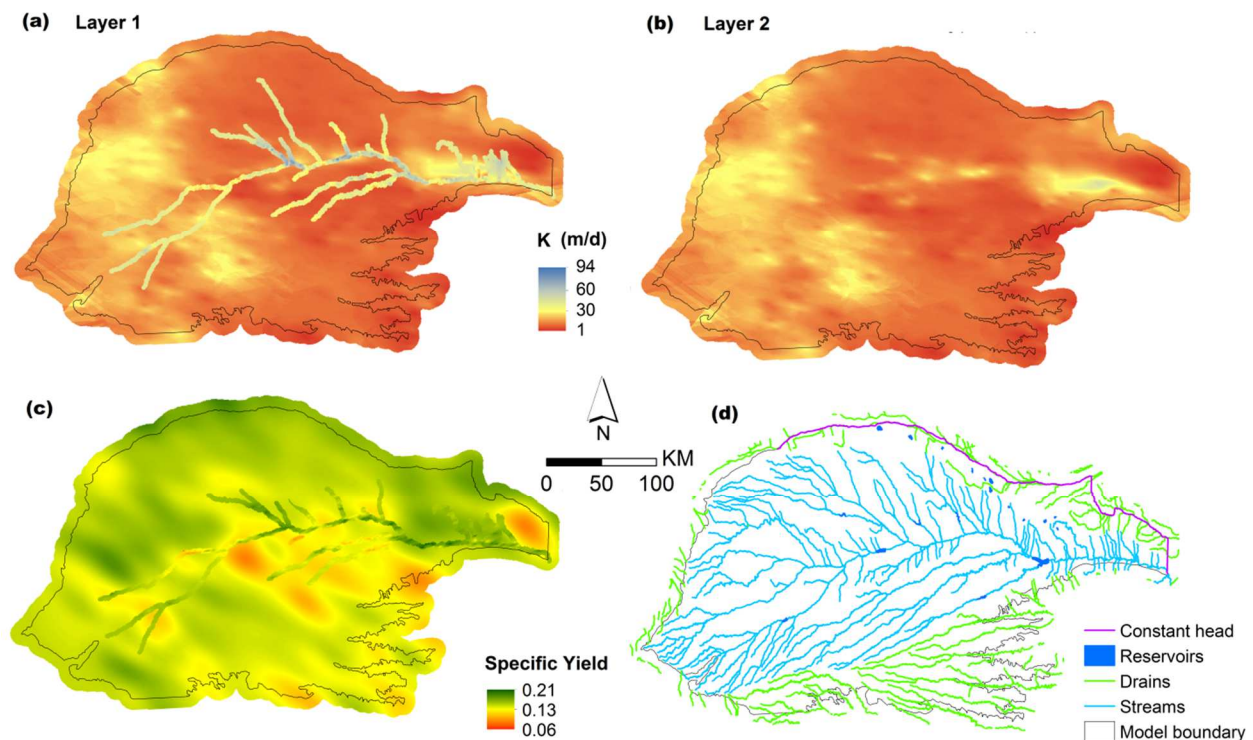


Figure 1.3: Maps of key model parameters. (a-b) Hydraulic conductivity of model layers (*high K is set for reservoirs*), layer 1 has separate interpolated K values for alluvial areas, (c) Specific yield of the first model layer (S_y of the second layer not shown here has only non-alluvial zone interpolated), and (d) groundwater model boundary conditions. Hydraulic conductivity and specific yield values were interpolated from point data using zonal (alluvial and non-alluvial zones) kriging. Stream and drain cells were simulated using the SFR2 and drain packages of MODFLOW, respectively.

Table 1.1 Zonal kriging models, parameters and predictions errors for K and S_y. *Semivariogram is used except where covariance is given, which means covariance variogram is used.*

| Zones | Models | Data Process | Lag size | Nugget | Parameters | | | R M S | R M S |
|-----------------------------|--|--------------|-------------|-------------|---|--------------|--------------|-------------|-------------|
| | | | | | Range | Partial Sill | Anisotropy | | |
| alluvial K | Simple | - | 1500 | 0.74 | 18000 | 0.20 | - | 24.7 | 0.98 |
| | Exponential | - | 3000 | 0.79 | 36000 | 0.17 | - | 24.6 | 0.97 |
| | Ordinary | - | 2000 | 0.75 | 15438 | 0.17 | - | 24.5 | 0.97 |
| | Exponential Simple Covariance Stable | - | 1000 | 0 | 12000 | 1.07 | - | 24.7 | 1.00 |
| Non alluvial K | Simple | Log | 3500 | 0.46 | 42000/ | 0.20 | 105.3 | 12.7 | 0.83 |
| | Exponential | Log | 2000 | 0.46 | 17369 17679/ | 0.27 | 5.4 | 12.7 | 0.83 |
| | Simple Stable | Log | 2000 | 0.44 | 5909 16656/ | 0.19 | 6.5 | 13.6 | 0.88 |
| | Ordinary Exponential | Log | 3500 | 0.46 | 42000/ 17369 | 0.20 | 105.3 | 12.8 | 0.92 |
| alluvial S _y | Simple | Log | 1000 | 0.66 | 7846/ | 0.19 | 76.8 | 5.3 | 1.02 |
| | Stable | Log | 2000 | 0.67 | 2627 9201/ | 0.19 | 77.0 | 5.3 | 1.02 |
| | | Log | 3000 | 0 | 3076 36000/ | 0.94 | 79.1 | 5.2 | 0.99 |
| | | Log | 3500 | 0 | 12086 42000/ 14071 | 0.95 | 78.9 | 5.2 | 0.99 |
| Non alluvial S _y | Simple | Log | 4500 | 0.13 | 54000/ | 0.67 | 119.0 | 4.3 | 0.99 |
| | Stable | Log | 4000 | 0.12 | 26976 48000/ | 0.67 | 117.8 | 4.3 | 0.99 |
| | | Log | 3800 | 0.12 | 25681 45600/ | 0.67 | 117.4 | 4.3 | 0.99 |
| | | Log | 3600 | 0.11 | 24625 43200/ 23861 | 0.67 | 116.4 | 4.3 | 0.99 |

The groundwater model was manually calibrated by adjusting the hydraulic conductivity and specific yield multipliers to spatial estimates of these parameters based on the USGS (Harbaugh et al. 2000, 2017). Root-mean-square-errors between domain-averaged annual simulated and observed water levels are shown in Table 1.2. Thus for the calibrated model, we use a K multiplier of 1.7 and a S_y multiplier of 0.7 because they achieve the minimum RMSE; model performance is shown in Figure 1.4 for different parameters.

Table 1.2 Model calibration.

| K multiplier | 0.9 | 1.1 | 1.2 | 1.5 | 1.6 | 1.7 | 1.8 | 1.9 | 2.0 |
|------------------|-------|-------|-------|-------|--------------|--------------|-------|-------|-------|
| RMSE | 0.461 | 0.398 | 0.368 | 0.294 | 0.287 | 0.281 | 0.282 | 0.283 | 0.292 |
| S_y multiplier | 0.25 | 0.4 | 0.5 | 0.6 | 0.7 | 0.8 | 0.9 | 1 | 1.1 |
| RMSE | 1.306 | 0.752 | 0.418 | 0.301 | 0.257 | 0.275 | 0.346 | 0.389 | 0.489 |

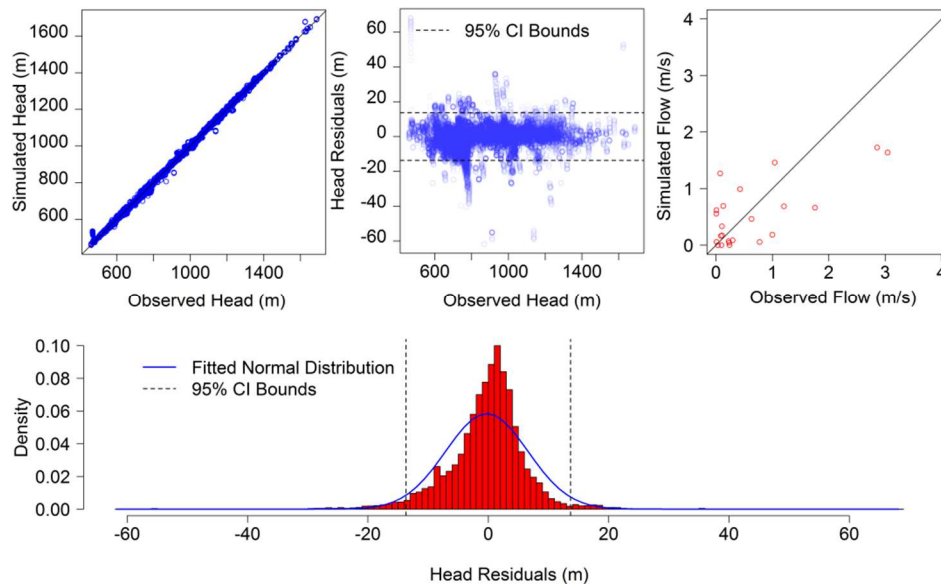


Figure 1.4: Simulated versus observed (a) water levels, (b) water levels residuals, and (c) streamflows.

1.2.3 Time-Varying Irrigation Area and Behavior

We use recent spatially-explicit estimates of annual remotely-sensed irrigation for the RRB region (Deines et al. 2017). The annual high-resolution (30 m) irrigation maps from 1999 to 2016 that were created using a random forest classification algorithm based on all available Landsat satellite imagery with climate and soil covariables in Google Earth Engine. These estimates show considerable interannual variability in irrigation location and extent with test data accuracies from 92% to 100% and R^2 from 0.88 to 0.96 relative to agricultural census information. We use these estimated irrigation maps to drive the annual irrigation extent in LHM. The LHM dynamic irrigation module (Figure 1.5) is triggered automatically during the growing season when soil moisture drops below a specified threshold and adds soil moisture. Specifically, irrigation is added if: (1) LAI exceeds the a threshold of crop development, and (2) there is a long enough delay since the last irrigation event, and (3) soil moisture is below a threshold. Each irrigation event then applies a specified amount of water. The application rate, or intensity of irrigation, is a function of the technology selected, pumping well capacity and irrigated field size; all which were evaluated with various scenarios.

Four scenarios were simulated: no irrigation, typical irrigation, high irrigation, and efficient irrigation. The efficient irrigation scheme was then compared with the irrigation observations to explore changes in irrigation efficiency through time. The high irrigation scenario applies parameters that fit observations from 2000 to 2004 to the 2005 to 2016 period. Based on estimated irrigation system yield and size of irrigation field across the High Plains Aquifer, the reduced irrigation scenario uses a 4 cm event max, 220 m³ per hour as irrigation system yield and 0.33 as

the fraction of plant available water to trigger irrigation (Kendall, A.D. 2009). Multiple irrigation scenarios were then simulated to evaluate parameters that represent efficient irrigation: 4 cm as event max, 0.33 as the fraction of plant available water to trigger irrigation and different irrigation system yields from 25- 480 m³ per hour with 2.2 to 33 days between events. Hydrologic responses in wet years (2008, 2009), dry years (2012, 2013), normal years (2006, 2010) and the 15-year-average (2002-2016) were examined to explore actual irrigation and its effects. Center pivot systems predominate irrigation technologies in Kansas Central High Plains in early years, which transitions into LEPA irrigation in later years (based on data from the Kansas Geological Survey). The specific locations in the RRB where center pivot and LEPA systems were adopted was unknown, thus we apply center pivot as the irrigation technology for the entire RRB, and evaluate the effects of different irrigation technologies by comparing the simulated irrigation with efficient irrigation.

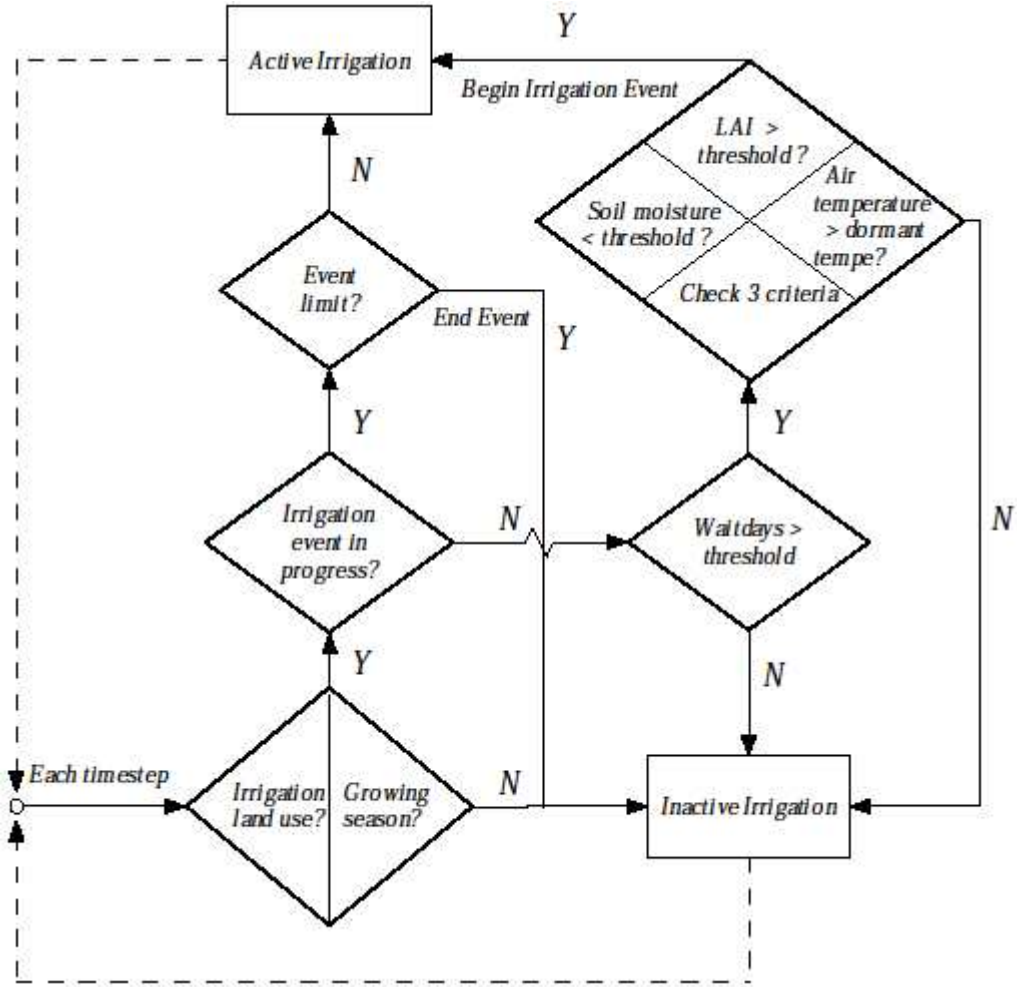


Figure 1.5: Diagram of the irrigation module framework.

1.3 RESULTS AND DISCUSSIONS

1.3.1 Calibration of Annual Irrigation Thresholds

The parameters specified for the dynamic irrigation model control its simulation for irrigation water and hydrologic responses, thus we calibrate these parameters based on experienced values and also the achievement of best fit to observed irrigation. For the RRB irrigation model, we used a soil moisture threshold method, which applies water when the sum of the soil moisture across the top three layers fell below a specified fraction of plant available water—defined as the difference between the permanent wilting point and field capacity. The soil moisture threshold was set to 0.33

for the efficient irrigation scenario. For all scenarios, water was applied during the growing season (120-235th day of the year). Based on the irrigation system and event estimated pumping water supply of agricultural land across the High Plains Aquifer (Kansas Geological Survey), irrigation system yield (yield of the water supply to the irrigation system) was set as 220 m³ per hour for the area of a typical irrigated field, which is 50 ha. The irrigation event maximum was set to 0.04 for the efficient scenario, and varied through time for the actual irrigation scenario.

Irrigation decisions are derived from a complex suite of conditions including soil moisture conditions and farmer decision strategies, which can be difficult to quantify. Thus to approximate actual irrigation conditions, we explored a variety of parameters and values to try to unravel this complexity. The two factors that we adjusted were the irrigation event maximum (maximum application per event) and soil moisture threshold parameters. These parameters were manually calibrated to best fit the RRCA irrigation data (See Table 1.3 for calibrated values). The irrigation event max was set as 0.045 m from 2000 to 2004, and 0.04 m from 2005 to 2016. The fraction of plant available water to trigger irrigation was set as 0.5, and the adjustment factor of this fraction was changed annually from 2000 to 2016 (Table 1.3, Figure 1.6b). The intention of this scenario is to best estimate actual irrigation parameters, using LHM as a climate-smart temporal disaggregation tool with amounts fit to the RRCA data. Based on the calibrated parameters, plant available water fraction is a relatively high steady number before 2009, and is declining annually afterward except dry years 2012 and 2013. Thus plant available water fraction along with irrigation event max identifies three different periods: 2000-2004, 2005-2008, and 2009-2016. The first period is steady high, the second steady medium, and the third low and decreasing.

Table 1.3 The adjustment factor of plant available water fraction for simulated irrigation.

| | | | | | | | | | |
|--------|-------|-------|-------|-------|-------|-------|-------|-------|-------|
| Year | 2000 | 2001 | 2002 | 2003 | 2004 | 2005 | 2006 | 2007 | 2008 |
| Factor | 1.362 | 1.159 | 1.348 | 1.141 | 1.344 | 1.198 | 1.287 | 1.28 | 1.324 |
| Year | 2009 | 2010 | 2011 | 2012 | 2013 | 2014 | 2015 | 2016 | |
| Factor | 1.126 | 1.12 | 1.096 | 1.266 | 1.168 | 1.038 | 1.062 | 0.952 | |

With the above calibrated parameters, we examine the model performance by comparing the spatial distributions of observed and simulated irrigation. Figure 1.6 shows domain averaged simulated versus observed regional irrigation and involved maps. The observed map was calculated as irrigation volume divided by the 1 mile observed cell size. The downscaled observed map was calculated as the observed irrigation volume divided by annual irrigation area estimates from Deines et al. 2017; values larger than 0.65 m were likely due to dividing by small aggregated irrigation areas, thus the values above 0.65 m are all mapped with the same color in the map.

In LHM, partial irrigation within a cell is not currently supported, which means one cell is either irrigated or not irrigated. Thus, to preserve total irrigated area, when the 30 m resolution irrigation map from Deines et al. (2017) is upscaled to the 600 m resolution model, cells with aggregated irrigation fraction smaller than a calculated threshold are set to non-irrigated, and those with a fraction greater than the threshold are set as irrigated. This threshold changes each year in response to the changing input irrigation data, but has a typical value of 0.45. Thus, the simulated irrigation map has fewer irrigation cells than the observed irrigation map (Figure 1.6c, d), but does preserve the total irrigated area.

Once LHM calculates irrigation water demand, it is extracted from the groundwater model using a spatially-variable ratio of surface water to groundwater sources. Recharge and irrigation

water applied from the LHM simulations were used to calculate net recharge. For the analysis of net recharge changes with irrigation, we assume all irrigation water is extracted from groundwater, since surface irrigation would be one value deducted from total irrigation in any year across the domain, which has no impacts to the net recharge trend with irrigation. When net recharge is supplied to groundwater model, the amount of the observed surface irrigation is necessary for simulations. The observed surface irrigation, about 5 to 22 percent of the total irrigation (RRCA, 2003), is used to estimate the annual pumping to the total irrigation ratio, therefore pumping water is simulated as the product of irrigation water applied and the annual pumping ratio. The difference of recharge and pumping water is the net recharge supplied to groundwater model.

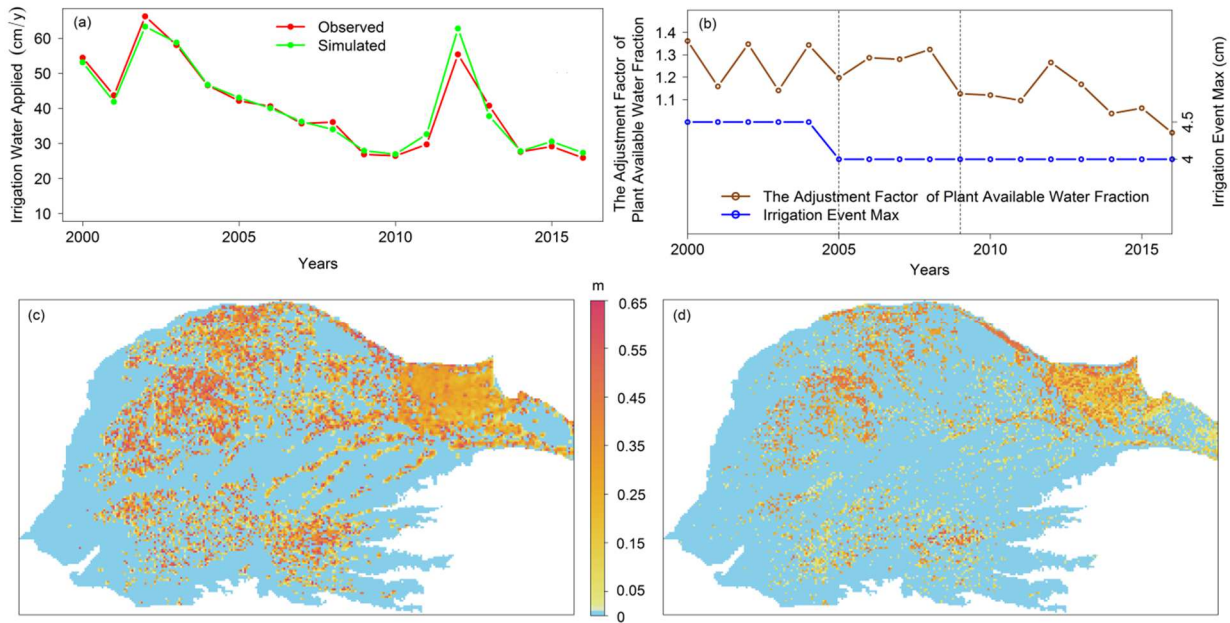


Figure 1.6: Simulated versus observed regional irrigation. (a) Domain averaged irrigation, (b) calibrated irrigation parameters, (c) down-scaled observed 15-year-average (2002-2016) irrigation map, and (d) simulated 15-year-average (2002-2016) irrigation map.

1.3.2 Hydrologic Changes due to Irrigation

With calibrated irrigation, the simulation estimates that this region has an average of 2.8 cm/y recharge, 2.0 cm/y runoff, and 51 cm/y ET from 2002 to 2015. Compared with the no irrigation scenario, an average of 12.6 % of the recharge comes from irrigation return flow. Model results also exhibit there are clear hydrologic changes in space and time due to irrigation. Figure 1.7 shows the 15-year-average simulated hydrologic change. Simulated return flow (Figure 1.7a) only occurs in irrigated lands. Sand dune areas in the northwestern portion of the domain have very low overland runoff (Figure 1.7b), while evapotranspiration (ET) (Figure 1.7c) tends to increase from west to east with a similar trend to precipitation. As expected, concentrated irrigated area in these sand dune areas has more return flow and a higher return flow to recharge ratio (Figure 1.7a, c), and less ET than in the lower hydraulic conductivity northeastern portion of the basin.

Hydrologic changes in time are also examined. The recharge simulated in LHM is the deep percolation delayed by flow to the water table. Figure 1.8 shows the simulated hydrologic changes due to irrigation through time. Irrigation return flow can continue throughout the year, but most is expected during the growing season (Figure 1.8a). There tends to be no clear difference of return flow between wet years and dry years, but the percentage of return flow over baseline recharge is lower in a wet year than a dry year, because baseline recharge is higher in a wet year (Figure 1.8b).

Irrigation appears to mainly affect overland runoff during the growing season, and the increased runoff by irrigation during earlier months of the growing season in dry years is larger than in wet years, related to higher irrigation applied during this period in dry years (Figure 1.8c). Based on these simulations, capturing runoff enhanced by irrigation may be a means to enhance

water resources, perhaps via artificial recharge.

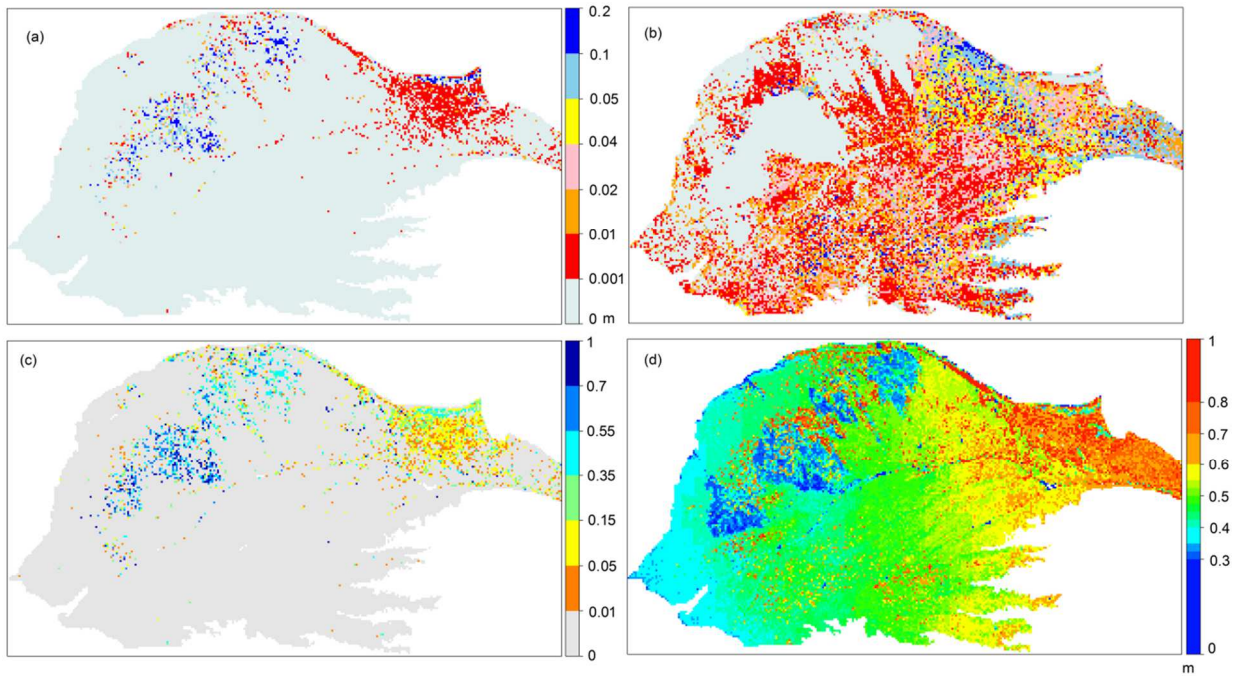


Figure 1.7: Maps of 15-year-average (2002-2016) simulated changes in: (a) return flow, (b) overland runoff, (c) return flow to recharge ratio, and (d) evapotranspiration due to estimated actual irrigation.

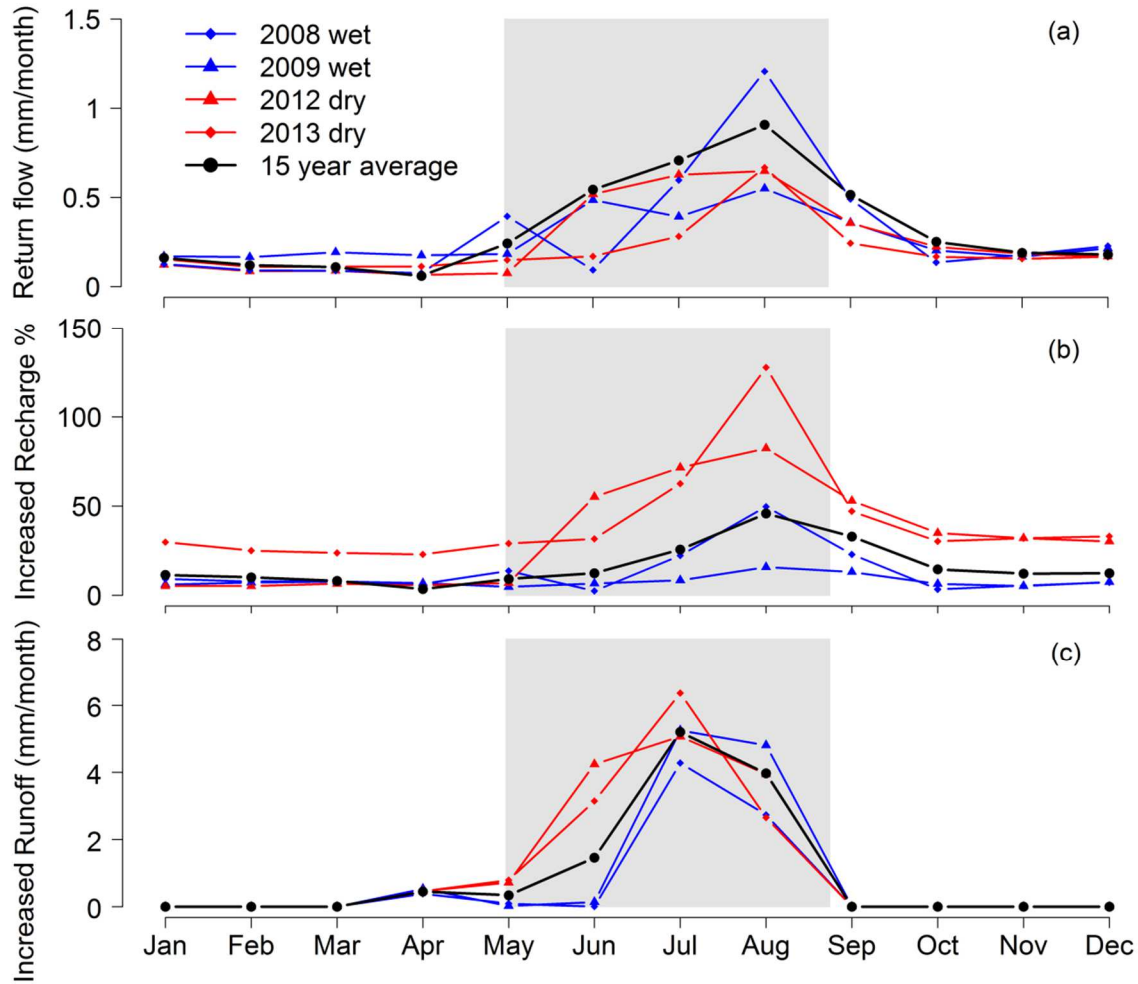


Figure 1.8: Simulated actual hydrologic change to actual irrigation across the domain. (a) Estimated monthly return flow, (b) increased percentage recharge with irrigation, and (c) increased overland runoff with irrigation. Grey areas indicate the growing season (120-235th day of the year).

1.3.3 Efficient Irrigation Range

The trend of hydrologic responses to different irrigation schemes contains large information that could provide a basis for irrigation strategies. The hydrologic components include water consumed by plants (transpiration), water reused in groundwater (return flow), water contributed to streamflow (runoff), and other sources that are trivial or insensitive to the change of irrigation. Thus we could evaluate efficient water use by stabilizing the crop water consumption and

minimizing the water loss to other sources under different irrigation scenarios. The irrigation scenarios that offer efficient water use therefore make up efficient irrigation range.

Based on these model results, we discussed the efficient use of: 1) runoff, 2) net recharge, and 3) transpiration changes. When irrigation water averaged over irrigated lands is applied below 20 cm/y, the simulations show very little overland runoff (Figure 1.9c), and the portion from irrigation is negligible in simulated streamflow (Figure 1.9b). When more than 20 cm/y of irrigation was applied in the simulations, overland runoff increases up to an irrigation threshold after which runoff rapidly rises. Above this threshold, irrigation efficiency is low, exhibited by the 1:1 slope, since any additional irrigation water effectively becomes overland runoff in the simulations. Below this threshold, a range of nearly constant overland runoff is formed, exhibiting a plateau. Also runoff is the major water loss since return flow will be reused and not counted as water loss. Thus, the efficient irrigation should not exceed the irrigation range with this nearly constant overland runoff. Dry years tend to have larger thresholds than wet years, as shown in Figure 1.9c & b. The runoff point (where runoff begins to increase) is also higher in dry years than the 20 cm/y of wet and normal years. As expected, irrigation appears to be more efficient in dry years than wet years due to less loss to overland runoff. In other words, if the same amount of irrigation is applied every year, farmers would waste more water in wet years, as excessive irrigation increased overland flow when rain falls on saturated fields.

Net recharge, which is the difference between recharge and applied irrigation water, starts to decrease once pumping starts in an irrigated area. The grey line is the 1:1 line, thus the vertical distance between the colored lines and the grey line is the simulated recharge for the analysis year

(Figure 1.9d). The positive relationship between recharge and irrigation is clear for the 15-year-average and the dry 2013 year. For the wet 2008 year, there are two peaks near 20 and 30 cm/y, which is one just before the runoff point and another within the efficient irrigation segment. In wet years, a smaller amount of irrigation could produce return flow compared with dry years. Return flow also rapidly rises when irrigation is just less than the runoff point and also within the range producing constant runoff, and this rapid increase is more obvious in wet years than dry years.

Net recharge over the domain decreases slowly, then declines suddenly at 20 cm/y irrigation (Figure 1.9 a), likely due to irrigation starting to flow overland to channels. Irrigation above 20-23 cm/y in dry years have negative net recharge, which means large areas have significant groundwater declines in dry years to meet crop water requirements. As long as the multiple-year-average is below 32.5 cm/y, net recharge average among the domain appears to be positive and the aquifer on average appears to be sustainable.

When irrigation water is applied at a higher rate, transpiration increases, and then reaches a plateau (Figure 1.9e). Maximum transpiration is reached at lower irrigation rates (about 22 cm/y) in wet years than dry years (> 33 cm/y). The transpiration maximum occurs when the crop requirement is met, and the irrigation range is the range with maximum transpiration without rapidly increased runoff.

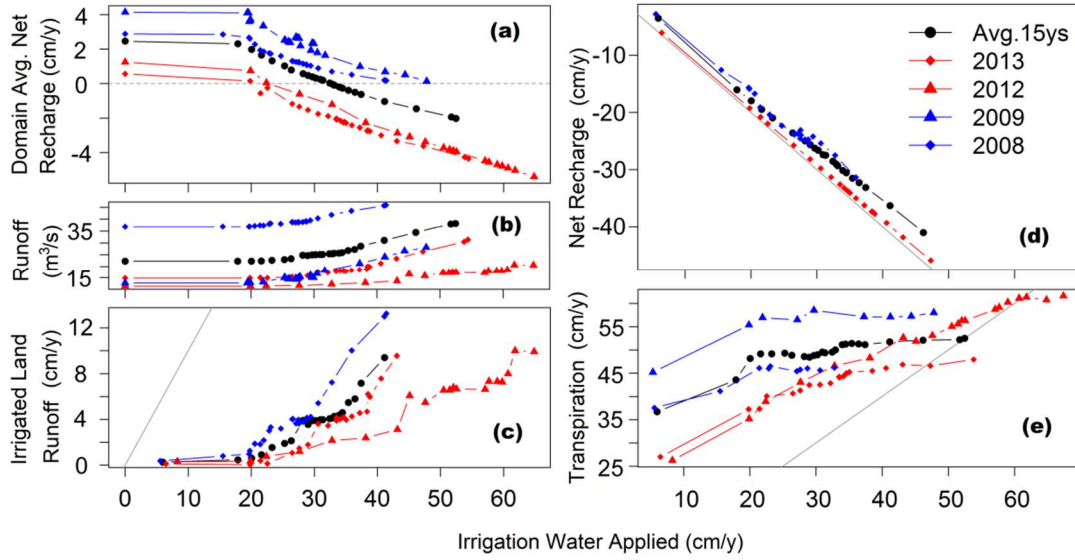


Figure 1.9: Hydrologic changes with different irrigation water. (a-b) Domain-average net recharge and overland runoff changes with irrigation, and (c-e) irrigated-land-average overland runoff, net recharge, and ET changes during the growing season to irrigation. (d) Recharge is the vertical distance between the colored lines and the grey 1:1 line; *the recharge of nearly zero irrigation (the first point) is proximate to natural recharge; return flow is the difference between recharge and the natural recharge.*

1.3.4 Irrigation Performance and Sustainability

Based on hydrologic changes across multiple irrigation scenarios, the efficient irrigation range tends to be 22-30 cm/y in wet year such as 2008, 34-38 cm/y in 2013 (dry), and an average of 22-35 cm/y from 2002 to 2016. The efficient irrigation range tends to be wider with smaller values in wet years than dry years (Figure 1.10a). The efficient irrigation range tends to be larger in normal years, because of significant increases in runoff threshold (less runoff loss) relative to wet years, and lower transpiration maximum (easier crop requirement met) relative to dry years. Observed irrigation depth was calculated by the RRCA observed irrigation volume and the updated irrigation maps (Deines et al., 2017). The observed irrigation is >40 cm/y before 2005, while the efficient irrigation range during this period is <40cm/y, nearly half of the observed

irrigation. The observed irrigation is 36.1 and 40.8 cm/y in 2008 and 2013 respectively, and 39.1 cm/y on average from 2002 to 2016. According to the efficient irrigation range, irrigation could have been reduced by 17 to 39 % in 2008, 7-17% in 2013, and 11-44% on average from 2002 to 2016. If the 15-year-average actual irrigation is reduced by about 18 % to 32 cm/y, the net recharge of the domain would likely be positive according to these simulations. Thus the reduced irrigation scenario takes the average 32 cm/y irrigation scenario with the 15-year-average net recharge around zero.

Observed irrigation after 2009 is similar to the reduced irrigation scenario, and also within the efficient irrigation range (Figure 1.10a). The trend of actual irrigation converged toward efficient irrigation. However, observed irrigation decreases while the efficient irrigation range increases in 2005 and 2006. The actual irrigation decreases while efficient irrigation range gently decreases in 2009. The same trend is exhibited with the calibrated parameters. Based on the calibrated parameters (Table 1.3, Figure 1.6b), farmers tend to apply less water per event after 2004 and appear to perform irrigation when soil moisture is below a lower threshold in more recent years. The decrease in observed irrigation is likely related to the increase of LEPA irrigation technology and groundwater pumping restrictions implemented to meet the compact by the US Supreme Court in 2004. It is also possible that the improved irrigation practices are means by which farmers meet their water use restrictions.

Water pumping is the amount required for groundwater-based irrigation based on the observed annual pumping ratio (Figure 1.10b). The reduced irrigation scenario has less irrigated area than baseline, thus baseline pumping over the domain is larger than the reduced pumping. Observed

irrigation tends to be unsustainable on average over the domain (Figure 1.10c). However, these simulations indicate that reduced irrigation rates for long periods may lead to much more sustainable irrigation practices over much of the domain.

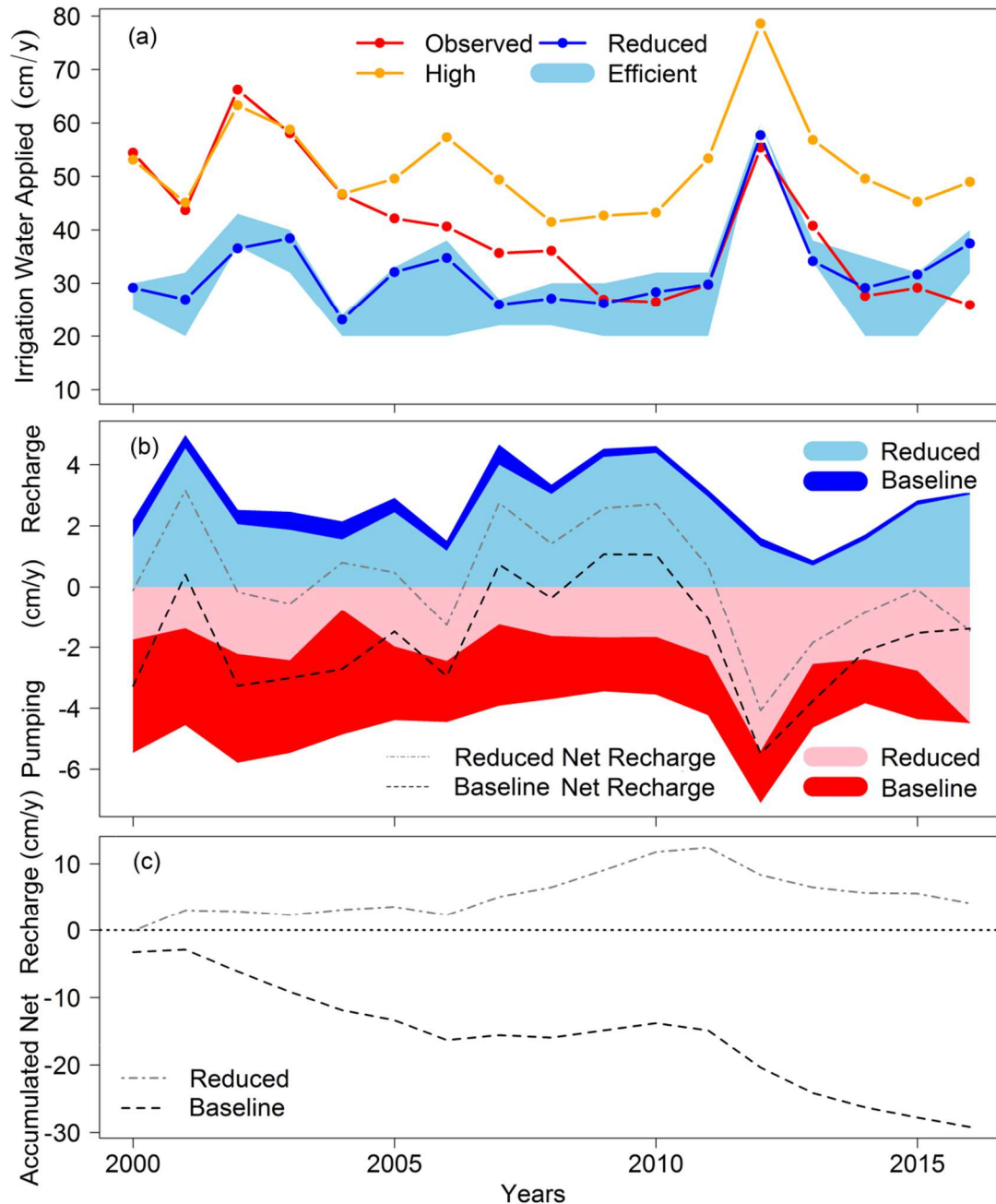


Figure 1.10: Reduced versus observed (a) irrigation water applied in the model, (b) water balance across the domain, and (c) accumulated net recharge across the domain. *Pumping water is the amount required for groundwater-based irrigation based on the observed annual pumping ratio.*

Domain-averaged water level changes for these simulations are shown in Figure 1.11. The baseline does capture the decreased water level changes through time, however it does not accurately represent the observed increase of water level changes from 2009 to 2012; this is likely impacted by the lower estimated irrigation in wet year 2008 (Figure 1.6a). In reality, higher irrigation was performed in 2008, which would reduce the water level changes in 2008, and produce more net recharge in the following year to enhance the water level changes after 2008. This delayed response of water level changes is also shown by comparing the observed water level changes to precipitation (Figure 1.1c). The observed water level changes are low in wet years 2008 and 2009, but high in 2010; and high in dry year 2012, but low in the next year. According to these simulations, groundwater level declines could be slowed across most of the domain by reducing irrigation rates by ~20% (Figure 1.12d). Although sustainable irrigation can be achieved on average across the domain by reducing irrigation over long periods (Figure 1.10 c), locally unsustainable irrigation in high irrigation areas cannot be eliminated by small reductions in irrigation (Figure 1.12c). Water resources enhancement, such as Aquifer Storage and Recovery, would likely be necessary in such areas to achieve sustainable water resources.

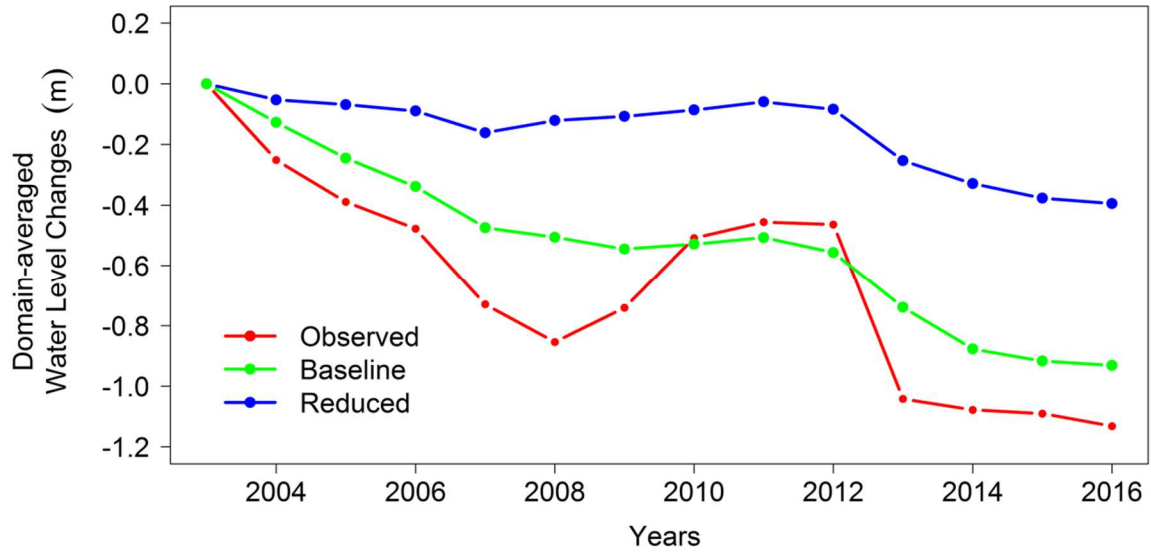


Figure 1.11: Domain-averaged water level changes based on 2003.

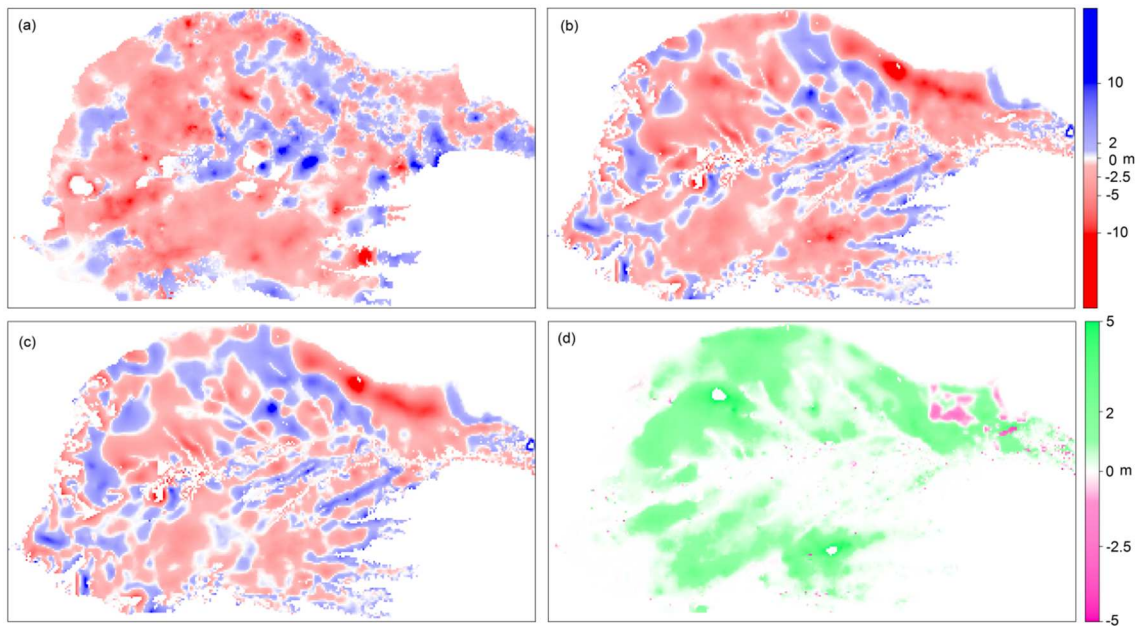


Figure 1.12: Maps of water level changes between 2016 and 2003. (a) Observed changes, (b) baseline, (c) reduced, and (d) simulated differences between reduced and baseline scenarios.

1.4 CONCLUSIONS

A two-layer high resolution integrated hydrologic model was built for the Republican River Basin that incorporates interactions between surface water and groundwater. Multiple irrigation

scenarios including the best estimate for irrigation practices and a reduced irrigation scenario are simulated to quantify hydrologic responses, and highlight the potential to achieve sustainable water levels in some areas by using more efficient irrigation practices.

Within the simulations that apply irrigation to supply crop water requirements, an efficient irrigation range exists within which crops have sufficient water and little water is lost to runoff. This efficient irrigation range is smaller in dry years than wet years. The 15-year- average efficient irrigation range for this region based on these simulations ranges from 22 to 35 cm/y from 2002 to 2016 in the Republican River Basin. According to the efficient irrigation range and Kansas Local Enhanced Management Areas (LEMAs), about 20 % reduction of the prior irrigation is possible without significant reductions in yield (Butler et al., 2016).

Compared with the temporal trend of efficient irrigation range, there are substantial decreases for the actual irrigation from 2005 to 2009. The efficient irrigation range increases in 2005 but observed irrigation rates decreased; observed irrigation rates from 2009 to 2016 were similar to the reduced rates indicating more efficient recent irrigation practices. Observed irrigation rates dropped to the efficient irrigation range since 2009 likely due to the combination of increasing application of LEPA irrigation technology and groundwater pumping restrictions to comply with the compact by the US Supreme Court in 2004.

According to our simulations, irrigation affects recharge throughout the year, while its effect on overland runoff is concentrated in the growing season. Irrigation affects recharge and overland runoff more during dry years than wet years. Return flow is frequently highest in August, while increased overland runoff due to irrigation is highest from July to August.

If the reduced irrigation is applied for an extended time period, the simulations indicate that water levels across much of the region would likely stabilize, and the decreasing trend of the domain-averaged water levels would begin to flatten out, thus much of system could likely be managed in a sustainable manner. Unfortunately some arid regions of the system cannot have sustainable irrigation without some form of enhanced recharge or imported water. Thus, we studied Aquifer Storage and Recovery in next Chapter.

REFERENCES

REFERENCES

- Ahmad M.D., H. Turrall, and A. Nazeer. 2009. Diagnosing irrigation performance and water productivity through satellite remote sensing and secondary data in a large irrigation system of Pakistan. *Agricultural Water Management* 96 (4): 551–64.
<https://doi.org/10.1016/j.agwat.2008.09.017>.
- Boucher, O., G. Myhre, and A. Myhre. 2004. Direct human influence of irrigation on atmospheric water vapor and climate. *Climate Dynamics* 22 (6-7): 597–603.
- Butler, J.J., Jr., D.O. Whittemore, B.B. Wilson, and G.C. Bohling. 2016. A new approach for assessing the future of aquifers supporting irrigated agriculture. *Geophysical Research Letters* 43(5): 2004-2010. <https://doi.org/10.1002/2016GL067879>.
- Cederstrand, J.R., and Mark F. Becker. 1998. Digital map of base of aquifer for High Plains aquifer in parts of Colorado, Kansas, Nebraska, New Mexico, Oklahoma, South Dakota, Texas, and Wyoming: U.S. Geological Survey Open-File Report 98-393
- Chow, Ven Te. 1959. Open channel hydraulics.
- Deines, Jillian M., Anthony D. Kendall, and David W. Hyndman. 2017. “Annual Irrigation Dynamics in the U.S. Northern High Plains Derived from Landsat Satellite Data.” *Geophysical Research Letters* 44 (18): 9350–60. <https://doi.org/10.1002/2017GL074071>.
- Garg, Amit, Bruce A. Kimball, and D C. Uprety. 2017. "Conservation Tillage." Conservation Tillage | ClimateTechWiki. N.p., n.d. Web. 14 Nov. 2017.
<<http://www.climatetechwiki.org/technology/conservation-tillage>>.
- Great Plains WATERS Network Observatory. 2014.
<http://gpobservatory.unl.edu/repubrivrbasin-backgrnd.shtml>, 5 September
- Gutentag, D.E., J.F. Heimes, N.C. Krothe, Richard R. Luckey, and John B. Weeks. 1984. Geohydrology of the High Plains Aquifer in parts of Colorado, Kansas, Nebraska, New Mexico, Oklahoma, South Dakota, Texas, and Wyoming. USGS Professional Paper 1400-B
- Guzha, A. C. 2004. Effects of Tillage on Soil Microrelief, Surface Depression Storage and Soil Water Storage. *Soil and Tillage Research* 76 (2): 105–14.
<https://doi.org/10.1016/j.still.2003.09.002>.
- Haacker, Erin M.K., Anthony D. Kendall, and David W. Hyndman. 2016. “Water Level Declines in the High Plains Aquifer: Predevelopment to Resource Senescence.” *Groundwater* 54 (2): 231–42. <https://doi.org/10.1111/gwat.12350>.

- Haddeland, I., D. P. Lettenmaier, and T. Skaugen. 2006. Effects of irrigation on the water and energy balances of the Colorado and Mekong river basins. *Journal of Hydrology* 324(1-4): 210–223. <https://doi.org/10.1016/j.jhydrol.2005.09.028>.
- Harbaugh, A.W., E.R. Banta, M.C. Hill, and M.G. McDonald. 2000. MODFLOW-2000, the U.S. Geological Survey modular ground-water model—User guide to modularization concepts and the Ground-Water Flow Process. USGS Open-File Report 00-92.
- Harbaugh, A.W., C.D. Langevin, J.D. Hughes, R.N. Niswonger, and L. F. Konikow. 2017. MODFLOW-2005 version 1.12.00, the U.S. Geological Survey modular groundwater model. U.S. Geological Survey Software Release, 03 February 2017, <http://dx.doi.org/10.5066/F7RF5S7G>
- Homer, C.G., J.A. Dewitz, L. Yang, S. Jin, P. Danielson, G. Xian, J. Coulston, N.D. Herold, J.D. Wickham, and K. Megown. 2015. Completion of the 2011 National Land Cover Database for the conterminous United States-Representing a decade of land cover change information. *Photogrammetric Engineering and Remote Sensing*. v. 81, no. 5, p. 345-354
- Houston, N.A., Gonzales-Bradford, S.L., Flynn, A.T., Qi, S.L., Peterson, S.M., Stanton, J.S., Ryter, D.W., Sohl, T.L., and Senay, G.B., 2013, Geodatabase compilation of hydrogeologic, remote sensing, and water-budget-component data for the High Plains aquifer, 2011: U.S. Geological Survey Data Series 777, 12 p., <http://pubs.usgs.gov/ds/777/>.
- Hyndman, David W, Anthony D Kendall, and Nicklaus R H Welty. 2007. Evaluating Temporal and Spatial Variations in Recharge and Streamflow Using the Integrated Landscape Hydrology Model (ILHM). In *Subsurface Hydrology*, 171:121–41. Geophysical Monograph Series. Blackwell Publishing Ltd. <https://doi.org/10.1029/171GM11>.
- Jiang Y., X. Xu, Q. Huang, Z. Huo, G. Huang. 2015. Assessment of irrigation performance and water productivity in irrigated areas of the middle Heihe River basin using a distributed agro-hydrological model, In *Agricultural Water Management*, 147: 67-81, ISSN 0378-3774
- Kendall, A.D. 2009. Predicting the impacts of land use and climate on regional-scale hydrologic fluxes. PhD diss., MICHIGAN STATE UNIVERSITY
- Konikow, Leonard F. 2013. Groundwater Depletion in the United States (1900 – 2008). *Scientific Investigations Report 2013 – 5079*, 75. <https://doi.org/10.1111/gwat.12306>.
- Kueppers, L. M., M. A. Snyder, and L. C. Sloan. 2007. Irrigation cooling effect: Regional climate forcing by land-use change, *Geophys. Geophysical Research Letters* 34, L03703. <https://doi.org/10.1029/2006GL028679>.
- Lobell, D. B., G. Bala, C. Bonfils, and P. B. Duffy. 2006. Potential bias of model projected

- greenhouse warming in irrigated regions, *Geophysical Research Letters* 33, L13709. <https://doi.org/10.1029/2006GL026770>.
- Lobell, David B., and Céline Bonfils. 2008. The Effect of Irrigation on Regional Temperatures: A Spatial and Temporal Analysis of Trends in California, 1934-2002. *Journal of Climate* 21 (10): 2063–71. <https://doi.org/10.1175/2007JCLI1755.1>.
- Luszcz, Emily C, Anthony D Kendall, and David W Hyndman. 2017. “A Spatially Explicit Statistical Model to Quantify Nutrient Sources, Pathways, and Delivery at the Regional Scale.” *Biogeochemistry* 133 (1). Springer Netherlands: 37–57. <https://doi.org/10.1007/s10533-017-0305-1>.
- Manfreda, S., M. Fiorentino, and V. Iacobellis. 2005. DREAM: A Distributed Model for Runoff, Evapotranspiration, and Antecedent Soil Moisture Simulation. *Advances in Geosciences* 2 (August 2016): 31–39. <https://doi.org/10.5194/adgeo-2-31-2005>.
- McGuire, V.L. 2009. Water-level changes in the High Plains Aquifer, predevelopment to 2007, 2005–06, and 2006–07. USGS Scientific Investigations Report 2009-5019. Reston, Virginia: USGS.
- MDA. 2011. Conservation Practices. Minnesota Conservation Funding Guide, Minnesota Department of Agriculture. Available at: <http://www.mda.state.mn.us/protecting/conservation/practices/constillage>.
- Niswonger, R.G., D.E. Prudic, G. Pohll and J. Constantz. 2005. Incorporating seepage losses into the unsteady streamflow equations for simulating intermittent flow along mountain front streams. *Water Resources Research* 41. <https://doi.org/10.1029/2004WR003677>.
- NLDAS. <https://ldas.gsfc.nasa.gov/nldas/>
- Peck, J.C. 2007. In: The Agricultural Groundwater Revolution: Opportunities and Threats to Development (pp 296-319). Wallingford, UK: CAB International.
- Pervez, M.S., J.F. Brown. 2010. Mapping Irrigated Lands at 250-m Scale by Merging MODIS Data and National Agricultural Statistics. *Remote Sensing* 2(10): 2388-2412. <https://doi.org/10.3390/rs2102388>.
- Pokhrel, Y. N., S. Koirala, P. J. F. Yeh, N. Hanasaki, L. Longuevergne, S. Kanae, and T. Oki. 2015. Incorporation of groundwater pumping in a global Land Surface Model with the representation of human impacts. *Water Resources Research* 51: 78–96. <https://doi.org/doi:10.1002/2014WR015602>.
- Myneni, R., Y. K. 2015. MCD15A3H MODIS/Terra+Aqua Leaf Area Index/FPAR 4-day L4 Global 500m SIN Grid V006. NASA EOSDIS Land Processes DAAC.

<https://doi.org/10.5067/modis/mcd15a3h.006>

- Ozdogan, Mutlu, Matthew Rodell, Hiroko Kato Beaudoin, and David L. Toll. 2010. "Simulating the Effects of Irrigation over the United States in a Land Surface Model Based on Satellite-Derived Agricultural Data." *Journal of Hydrometeorology* 11 (1): 171–84. <https://doi.org/10.1175/2009JHM1116.1>.
- Pei, Lisi, Nathan Moore, Shiyuan Zhong, Anthony D. Kendall, Zhiqiu Gao, and David W. Hyndman. 2016. Effects of Irrigation on Summer Precipitation over the United States. *Journal of Climate* 29 (10): 3541–58. <https://doi.org/10.1175/JCLI-D-15-0337.1>.
- RRCA (Republican River Compact Administration). 2003. Groundwater model documentation. Online at <http://www.republicanrivercompact.org>.
- Schaaap, Marcel G., Feike J. Leij, Martinus Th. van Genuchten. 2002. A Computer Program for Estimating Soil Hydraulic Parameters with Hierarchical Pedotransfer Functions. *Journal of Hydrology* 251 (1980): 163–76.
- Soil Survey Staff, Natural Resources Conservation Service, United States Department of Agriculture. Web Soil Survey. Available online at <https://websoilsurvey.nrcs.usda.gov/>.
- Taghvaeian, S. and C. M. U. Neale. 2011. Water balance of irrigated areas: a remote sensing approach. *Hydrological Processes* 25: 4132–4141. <https://doi.org/10.1002/hyp.8371>
- U.S. Department of Agriculture, and National Agricultural Statistics Service. 2012. Conservation Producers Protect or Improve Millions of Acres of Agricultural Land. 2012 Census of Agriculture Highlights, 1 July 2014.
- U.S. Department of Agriculture, and National Agricultural Statistics Service. 2012. "Nebraska" 2012 Census of Agriculture States Profile.
- U.S. Fish and Wildlife Service. 2014. <https://www.fws.gov/wetlands/index.html>
- U.S. Geological Survey. 2011. High Plains Water-Level Monitoring Study, <http://ne.water.usgs.gov/ogw/hpwlms>, accessed 5 September 2014.
- U.S. Geological Survey. 2014. Equus Beds Groundwater Recharge Project, <http://ks.water.usgs.gov/equus-beds-recharge>
- U.S. Geological Survey water use data. <https://waterdata.usgs.gov/nwis/wu>.
- Whittemore, D.O., J.J. Jr. Butler, and B.B. Wilson. 2016. Assessing the major drivers of water-level declines: New insights into the future of heavily stressed aquifers. *Hydrological Sciences Journal* 61 (1): 134-145. <https://doi.org/10.1080/02626667.2014.959958>.

- Wiley, M.J., D.W. Hyndman, B.C. Pijanowski, A.D. Kendall, C. Riseng, E.S. Rutherford, S.T. Cheng, M.L. Carlson, J.A. Tyler, R.J. Stevenson, P.J. Steen, P.L. Richards, P.W. Seelbach, J.M. Koches, and R.R. Rediske. 2010. A multi-modeling approach to evaluating climate and land use change impacts in a Great Lakes river basin. *Hydrobiologia* 667 (1): 243-262. <https://doi.org/10.1007/s10750-010-0239-2>.
- Zeng, R., and X. Cai. 2014. Analyzing Streamflow Changes: Irrigation-Enhanced Interaction between Aquifer and Streamflow in the Republican River Basin. *Hydrology and Earth System Sciences* 18 (2): 493–502. <https://doi.org/10.5194/hess-18-493-2014>.

CHAPTER 2 POTENTIAL OF AQUIFER STORAGE AND RECOVERY

2.1 INTRODUCTION

Artificial recharge hereafter “ASR” (aquifer storage and recovery), involves enhancing the amount of water entering a groundwater reservoir. This includes direct recharge through injection or drainage wells, pits, and spreading basins. Since the early 1900s, there has been interest in using drainage wells to reclaim wetlands and dispose of water from storm runoff and sewage. With the seasonal water imbalance exacerbated by increasing water demand, a variety of ASR techniques have been implemented to enhance recharge for many groundwater source regions (Weeks 2002; Basagaoglu and Marino 1999; Bloyd 1971). Excess surface water can be stored in aquifers that have available storage and recovered during drought or high demand periods. ASR is also called conjunctive water management.

ASR has been practiced in multiple regions of the US. ASR of storm runoff by spreading basins has been practiced on Long Island since the 1930s, and wells have been proposed to inject water to recharge basalt and alluvial aquifers in Washington, Oregon, and Idaho (Weeks 2002; Koch 1984; Hamlin 1987). Reclaimed water has been spreading to replenish groundwater in the Montebello Forebay area, Los Angeles, California since 1962. The Water Factory 21 project in Orange County, California was the first injection project that uses highly treated municipal wastewater as a water supply; it has been in operation since 1976 (U.S. National Research Council 1994). The Bear Canyon Recharge Project was the first to receive a full-scale Underground Storage and Recovery (USR) permit in New Mexico to release bank-filtered surface water into an arroyo during the winter months (Fleck 2014). Approximately 333 ASR wells have been

implemented as part of the Comprehensive Everglades Restoration Plan for the region and other water systems in Florida (U.S. Army Corps of Engineers 2015). Worldwide, over 100 ASR facilities are operating, ranging from pilot projects to full-scale operations (EPA 2016).

For large agricultural regions, ASR could also be performed via existing ditch-furrow systems in periods with unallocated surface water flow. For example, a canal leakage study in Scottsbluff, Nebraska argued that leakage water should be considered a beneficial and reasonable use, since it recharges the local aquifer (Harvey and Sibray 2001); the alternative of lining canals to reduce leakage would result in groundwater level declines across the region adjacent to and beneath the canals. A 10-year study in Uttar Pradesh, India found that surplus monsoon water can recharge aquifers on a large scale, providing farmers with more crop security. The water table in this region has risen by over 5.5 meters and farmers benefited from the corresponding reductions in pumping costs and improved cropping patterns with increased incomes of ~26%. Such research suggests that modifying the operation of unlined irrigation systems to carry surplus flows is an effective way to recharge groundwater in areas with similar hydrogeological conditions (IWMI-Tata Water Policy Program 2002). Another modeling study found that regional recharge could be enhanced by 7 to 13% via agricultural managed aquifer recharge through canal seepage and off-season field irrigation in a semiarid agricultural basin of the western US (Niswonger et al. 2017).

ASR studies can be grouped into research studies and site-specific water resource studies. Among the studies of potential sites, ASR performance has been explored using field experiments and numerical models, including approaches to monitor and simulate water quality changes (Antoniou et al. 2013; Bakker 2010; Vanderzalm et al. 2013; Ward et al. 2009). The recharge

component of ASR utilizes spreading basins and injection wells, while extraction wells are generally used to recover the stored water. Studies that examine efficiency improvements often focus on mechanisms like colloidal transport through porous media, and developing technologies to avoid well clogging, improve recharge rates, and protect fresh groundwater from saltwater (Signor et al. 1970; Zurbier et al. 2014; Händel et al. 2014). Multiple simulation-optimization approaches for conjunctive management have maximized water storage on the surface and in the subsurface (e.g., Mosch 1998; Philbrick and Kitanidis 1998; Lowry and Anderson 2006; Hernandez et al. 2014).

The performance of ASR sites is affected by many factors, thus hydrologic characterization is important to evaluate ASR viability for each potential site (Phillips 2002), focusing on quantifying the conditions that control the ability of water to be recharged and later extracted from the aquifer. It is also important to characterize the hydraulic gradient along potential conveyance structures to calculate the costs for ASR water delivery and to quantify potential flow losses back to rivers in the groundwater system. Elevation differences and distances to pump water determine the power costs, which need to be accounted for in a cost benefit analysis. Available land uses also need to be considered to minimize potential environmental impacts (Brown 2005). Forested or wooded lands are important habitats that should generally not be developed as ASR sites, and urban developed areas and polluted areas such as landfills are not available. Methods to evaluate the potential of ASR sites commonly overlay a series of maps to combine planning factors including hydrologic, geologic, and landscape factors, along with the locations of threatened or endangered species (Focazio et al. 2002; Brown et al 2005). Once ASR sites are selected, water could be artificially

recharged to groundwater by some combination of surface and subsurface methods.

Surface ASR methods include flooding, spreading basins, percolation tanks, stream retention, and ditch-furrow systems. Subsurface methods include recharge pitch/shafts, injection wells, dry wells, wet wells, and dug wells. Combination methods include spreading basins plus recharge wells or pitch/shafts. If the stream bed has high hydraulic conductivity, induced recharge could be performed by pumping from groundwater near the river and delivering it to areas with significant drawdown via canals or pipes.

Designing appropriate ASR techniques for a region involves a detailed analysis of advantages and disadvantages of each method. When land price is low, surface application methods are generally much more cost-effective than subsurface methods. However, surface methods are limited by acceptable topography and land uses (Ankit Saini 2015), plus there can be substantial losses of water by evapotranspiration. Flooding requires large regions with nearly flat topography. High conductivity soils are needed to achieve adequate vertical infiltration, thus spreading basins are generally found in alluvial areas and regions with highly fractured and weathered rocks. Installation of low head or check dams can enhance stream retention in areas with permeable formations below the channel. Ditch and furrow systems are commonly feasible in regions with irregular topography. Subsurface methods have minimal restrictions of available area, topography or land use, with negligible water losses, however water treatment and electricity can add substantial costs. Well clogging was also a major issue with injection well systems, however in some cases clogging may be relieved by water recovery operations using the same wells for extraction. Based on cost estimates and topographic conditions, appropriate ASR techniques can

be designed after potential sites are identified.

There are significant concerns about long-term water availability over the High Plains Aquifer, thus there have been extensive ASR studies in Kansas, Nebraska, Colorado, and South Dakota (Gillespie and Slagle 1972; Gillespie et al. 1977; Prill 1977; Taylor 1975; Emmons 1977, 1987; Lichtler et al. 1980; Sumner et al. 1991). In 1984, the High Plains Groundwater Demonstration Program started, with projects to demonstrate ASR potential in 17 western states spanning a variety of hydrogeological conditions, including three in the High Plains Aquifer. The Wood River and York Projects in Nebraska were completed before 1998 and the Equus Beds Project in Kansas was tested for ASR between 1995 and 2005, with active ASR activities after 2007 (Ziegler et al. 2010). The Kansas Water Office has conducted research on the potential to draw water from the Missouri River during high flow periods, however the costs of constructing a reservoir and piping water to users is high (Carpenter 2015). Such demonstrations may show that ASR provides a cost effective way to capture and store available water for regions where heavy irrigation pumping from groundwater has resulted in significant water level declines. As discussed in Chapter 1, some arid regions overlying the HPA cannot support sustainable irrigation without enhanced recharge or imported water. Thus we explore potential sites across the High Plains Aquifer where water table declines could be at least partially relieved, and more specifically how much impounded water could be stored via ASR across the Republican River Basin.

2.2 METHODS

Water management strategies including ASR would be useful in areas where there have been large water table declines since predevelopment. The central idea of water use and management is

water relocation. Although irrigation with a surface water source can enhance groundwater recharge, most irrigation across the High Plains Aquifer uses groundwater as its source. For such regions, ASR can be an effective water management strategy in which surface water is relocated back to groundwater.

By 1940, extensive water level data was available from wells across the High Plains Aquifer (HPA), thus interpolated water table maps can be relatively accurate (Haacker et al. 2016, McGuire 2012). We use the 250 m interpolated water table maps from Haacker et al. (2016) as our data source for this research. We then used daily discharge data from USGS gaging stations to evaluate water availability, since streamflow is the primary potential water source for ASR.

2.2.1 Water Availability of Potential ASR Sites

We calculated the potential water availability for ASR, using a minimum streamflow threshold. There is no established minimum streamflow requirement in HPA states except Kansas, which established monthly Minimum Desirable Streamflow (MDS) values (Kansas Water Appropriation Act 1984). Given the importance of minimum flows, we applied the ratio of MDS to monthly average (1997 to 2016) discharge from a Republican River site near the Nebraska-Kansas (NE-KS) boundary to the HPA region as the standard for ASR water diversion. MDS in Kansas was established between 1984 and 1990 with the historical discharge data to enhance baseflow for instream water uses (Jackson 2009). We chose to base our ASR water estimates on streamflow data from 1997 to 2016 because flows were higher than the prior two decades, thus this provides a conservative estimate. This ratio of monthly flow to MDS is 1.75, 1.69, 2.08, 2.70, 4.35, 4.76, 2.70, 2.22, 2.70, 2.63, 2.17, and 2.17 from January to December. Here, we assume that streamflow

above the MDS values could be used for ASR.

Potential High Plains Aquifer ASR sites were explored within 5 kilometer buffered areas of streams. This distance was determined based on earlier studies that indicated the distance to source water must be less than 5 km to improve the cost effectiveness of moving water (Brown et al 2005). Detailed cost benefit analysis could quantify the economics associated with different distances, but this is beyond the scope of this study.

In addition to the 5 km buffered areas along the river, the existing canal system across the HPA provides potential conveyance for ASR water; new canals could also be built to move water along contour lines. Water could also be transferred from further distances to the high demand areas. To evaluate long-distance water transport in the Republican River Basin, we interpolated flow between observed streamflow at USGS gages along streams using the ARCGIS flow accumulation paths (Figure 2.1). No flow is assumed for the upstream most point of a stream (Figure 2.1b).

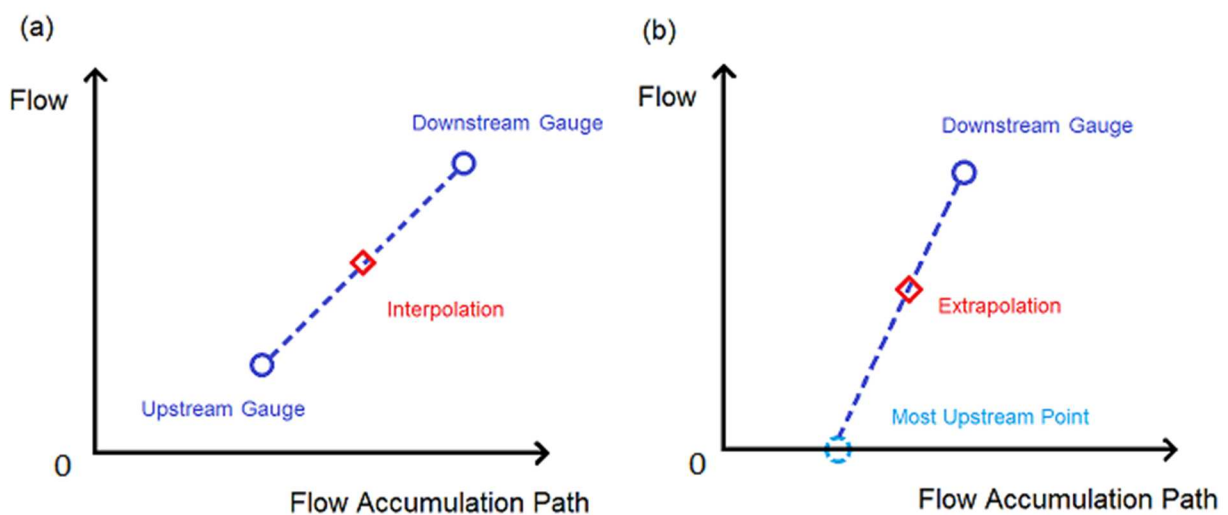


Figure 2.1: Conceptual diagram of flow (a) interpolation, and (b) extrapolation. *The most upstream point of a stream from the flow accumulation grid is assigned zero flow.*

2.2.2 Criteria for Potential ASR Sites

The aquifer hydraulic conductivity and groundwater level gradients toward rivers control the distribution and fate of injected water. Aquifers with low hydraulic conductivity would generally not be chosen for ASR because of the limits this poses to recharge and extract large volumes of water. Brown (2005) used a minimum saturated zone transmissivity for ASR recovery of $> 93 \text{ m}^2/\text{d}$ ($1000 \text{ ft}^2/\text{d}$), and a minimum saturated thickness of ~ 8 meters. Based on this analysis, we excluded areas with lower predevelopment saturated thickness transmissivity for ASR consideration; other thresholds could be determined based on a number of factors including economics. The saturated zone thickness was calculated by subtracting the 2015 groundwater levels from the DEM elevations (Haacker et al. 2016). Hydraulic conductivity values for this study were based on Gutentag et al. (1984), which were assigned based on drillers' logs with lithologic descriptions.

According to Brown (2005), hydraulic gradients for ASR should be less than 0.001 to minimize groundwater flowing to other areas where it is not readily extractable. However, high gradients are not a concern when they exist due to cones of depression from extensive pumping, as this could allow recharged water to be redistributed to the high water-demand areas. This is the case for most of the HPA region (Figure 2.2), thus we removed the consideration of hydraulic gradient constraint from our analysis. To minimize the loss of ASR water back to rivers via groundwater flow, potential ASR sites in this study are limited to areas near losing rivers. According to our analysis, most of the Little Arkansas River, where the current operating ASR project in the HPA-the Equus Beds ASR project site is located, also loses surface water to groundwater. Losing river reaches were identified as those where groundwater levels in the

vicinity of streams are below the surface elevation based on the DEM from the National Elevation Dataset. They are calculated using land surface elevation (NED); water table elevations were resampled to the 26 m DEM cells using the nearest-neighbor approach based on the 250 m kriged water table map from Haacker et al. (2016). Due to the groundwater level declines in the HPA region, many more river reaches are now losing water to groundwater according to the water level maps since predevelopment. As a result, there is an increasing potential of ASR through time in such regions.

Acceptable land use types for ASR were screened from the 2011 National Land Cover Database, as barren, herbaceous, and planted/cultivated classes (Brown et al 2005). Here we define “Natural storage” (Figure 2.3) to be the storage space between the predevelopment and 2015 water table elevations. Because it is part of the natural aquifer storage volume which has been lost due to aquifer development. The saturated aquifer material is assumed to be vertically consistent across the alluvial zone or non-alluvial zone, thus for the natural storage zone that we defined here, we use the alluvial or non-alluvial hydraulic conductivity and specific yield, depending on which zone contains the natural storage zone. A 2.5 m zone below the DEM was removed from the storage zone as this shallow zone could result in loss of water via evapotranspiration and salinization. Thus within the natural storage zone, we assume no loss to surface water.

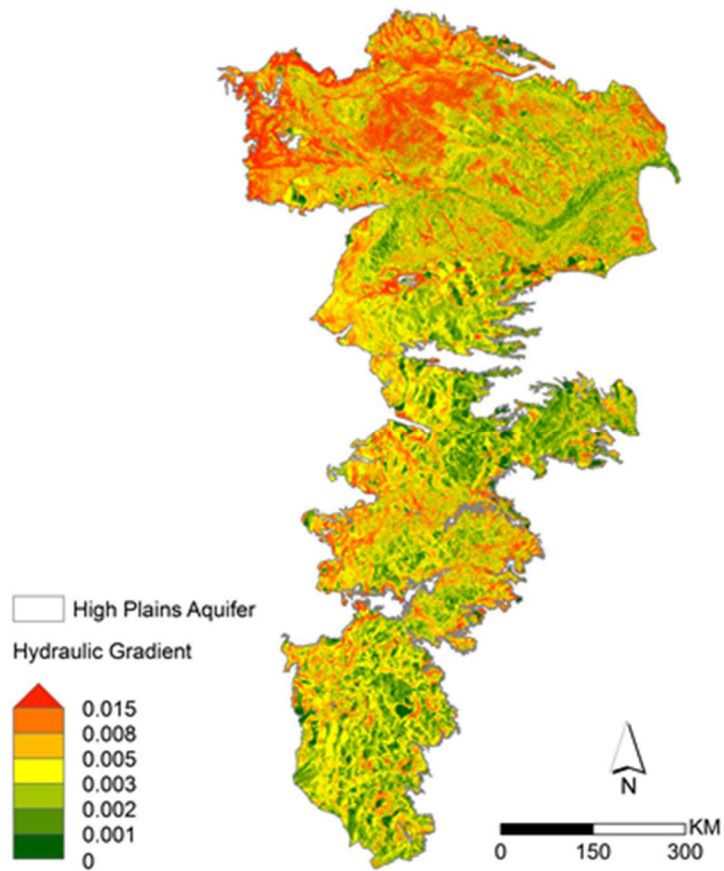


Figure 2.2: Hydraulic gradient map of the High Plains Aquifer in 2015. *(Calculated based on 2015 water table elevation maps from Haacker, et al 2016).*

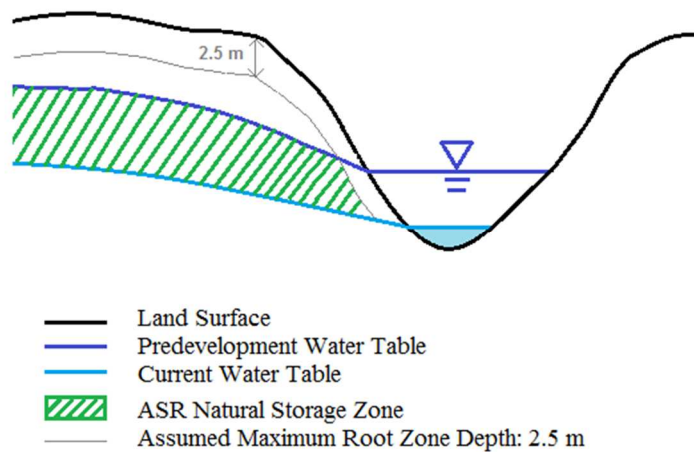


Figure 2.3: Conceptual diagram of the ASR natural storage zone.

Potential ASR sites for the HPA region were selected by overlaying the natural storage thickness map with acceptable transmissivity, saturated thickness, and land use. Potential ASR sites would likely be within 5 km buffers of losing rivers, considering transport costs. However, potential ASR sites are also evaluated in the Republican River Basin including sites that would involve long-distance water transport.

2.3 RESULTS AND DISCUSSIONS

2.3.1 Potential ASR Sites across the HPA

Several regions across the Central and Southern HPA could greatly benefit from ASR projects given the extensive declines in groundwater availability due to long term groundwater pumping for irrigation at rates that greatly exceed recharge (Haacker et al. 2016). The geologic conditions across much of the HPA region appear to be appropriate for ASR (Figure 2.4a). Several regions appear to have sufficient streamflow for ASR in the central High Plains while the southern High Plains rarely has sufficient water for such practices (Figure 2.4b). An example of an operational ASR project is the Equus Beds, located in the eastern portion of the central High Plains.

The northern regions of the northern High Plains have large volumes of water that could potentially be used for ASR, however there is limited need or natural storage space since water levels have been relatively stable in that region. Most of the arid western Northern High Plains has low transmissivity and saturated thickness for water recovery (Figure 2.4a).

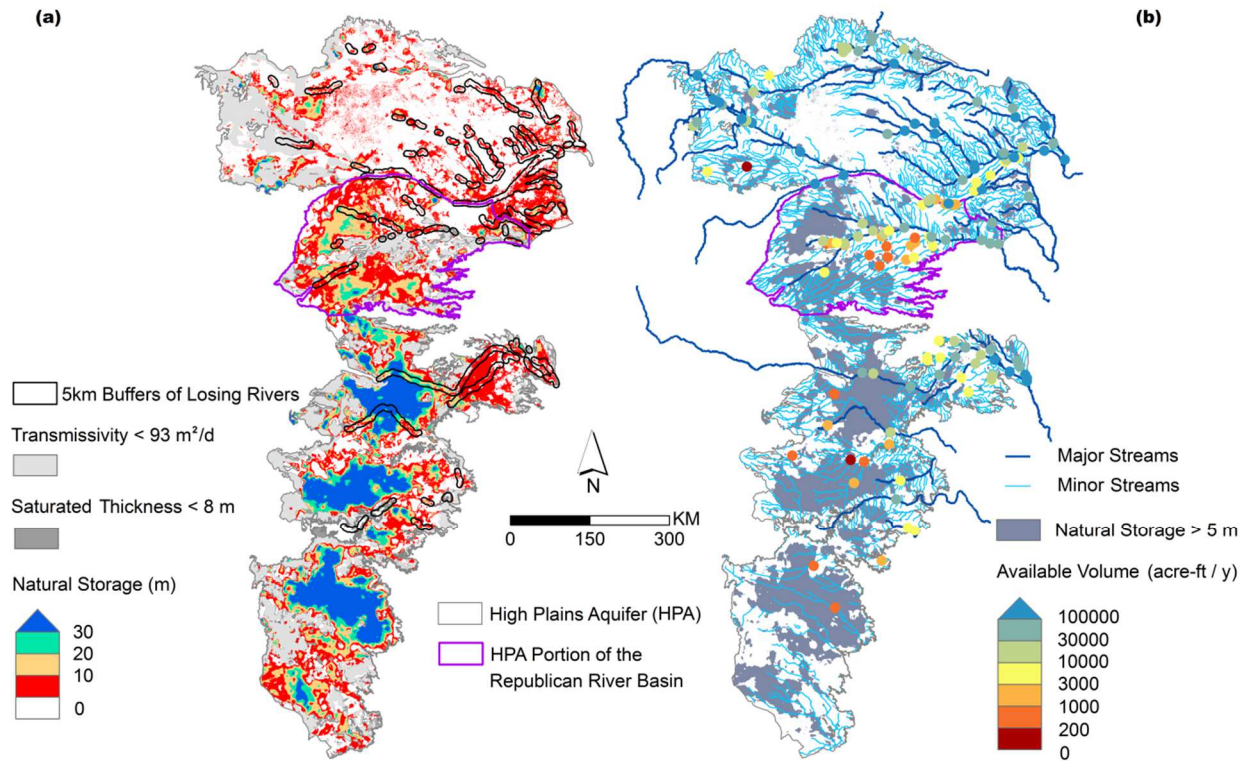


Figure 2.4: Estimated ASR potential in the High Plains Aquifer includes analysis of: (a) current natural storage thickness (*Calculated based on 2015 water table elevation maps from Haacker, et al 2016*), and (b) average available water volumes for potential ASR sites from 1997 to 2016. *Natural storage is not shown where transmissivity < 93m²/d and saturated thickness < 8 m, because these areas likely do not have sufficient potential for ASR due to ineffective storage and recovery. Most areas with saturated thickness < 8 m also have transmissivity < 93m²/d, thus the overlapped area is not shown in the figure. Available water is defined as the streamflow minus the in-stream use; the Republican River Compact regulations are used later relative to the total streamflow at the NE-KS border.*

2.3.2 Potential ASR Sites in the Republican River Basin (RRB)

A map of natural storage thickness for potential ASR in the RRB (Figure 2.5a) shows large natural storage areas available in the western portion of the basin. Tributaries in the northwestern portion of this region are close to the North Platte River, which has available water that exceeds existing water rights (Figure 2.4b). If water were to be transferred from the North Platte River to these tributaries, drawdown in the northwestern portion of the basin could likely be relieved.

This idea is promising because water could be pumped a short distance from the Platte River and discharged to tributaries of the Republican River. During low flow periods, this would likely provide a much lower cost alternative than the Nebraska Cooperative Republican Platte Enhancement project (N-CORPE) that currently extracts groundwater, which is discharged to the Republican River to meet the requirements of the Republican River Compact. During high flow periods, the diverted Platte River water could be used for ASR. Available water from other portions of the basin could also be used for ASR and offset by Platte River water.

An important characteristic for ASR sites is water storage depth (Figure 2.5b), which we calculated as the product of natural storage and specific yield (Houston et al. 2013) and then interpolated by zonal kriging from point data. The 50-meter interval contour lines are marked with thick solid lines, while 10-meter ones with thin dashed lines. The path of diverted water via gravity flow would require canal slopes of 1:4000 to 1:2000 (Thandaveswara 2017). The longest contour line in the RRB map is about 300 km, thus the canal would drop 15 m in elevation with a 1:2000 slope along its length. Thus some potential ASR sites far away from the Republican River could potentially be supplied with available water via canals or pipelines with gravity drainage. Average storage area is defined as the average extent where water declines could be relieved by ASR. It is calculated as available water divided by estimated storage water depth. With 1 m stored water depth, the possible area that could be used for ASR storage is 3.1-11.7 km² in northwestern portion of the basin, and 1.5-3.1 km² in southwestern portion (Table 2.1). Table 1 shows the extent where water declines could potentially be relieved by ASR. The streamflow into Kansas on the Republican River averaged 127,890 acre-feet per year from 1997 to 2016. If all the available water

was taken for potential ASR upstream of the eastern-most gauge in Figure 2.6, the discharge flowing into Kansas would likely decrease by 36% to 81,259 acre-feet per year. Since Nebraska had to pump groundwater to meet the water requirement of the Republican River Compact (Deines et al. 2017), available water from the Republican River may not be used for ASR without decreases in irrigation water use or transferring water from Rivers outside the basin such as the North Platte.

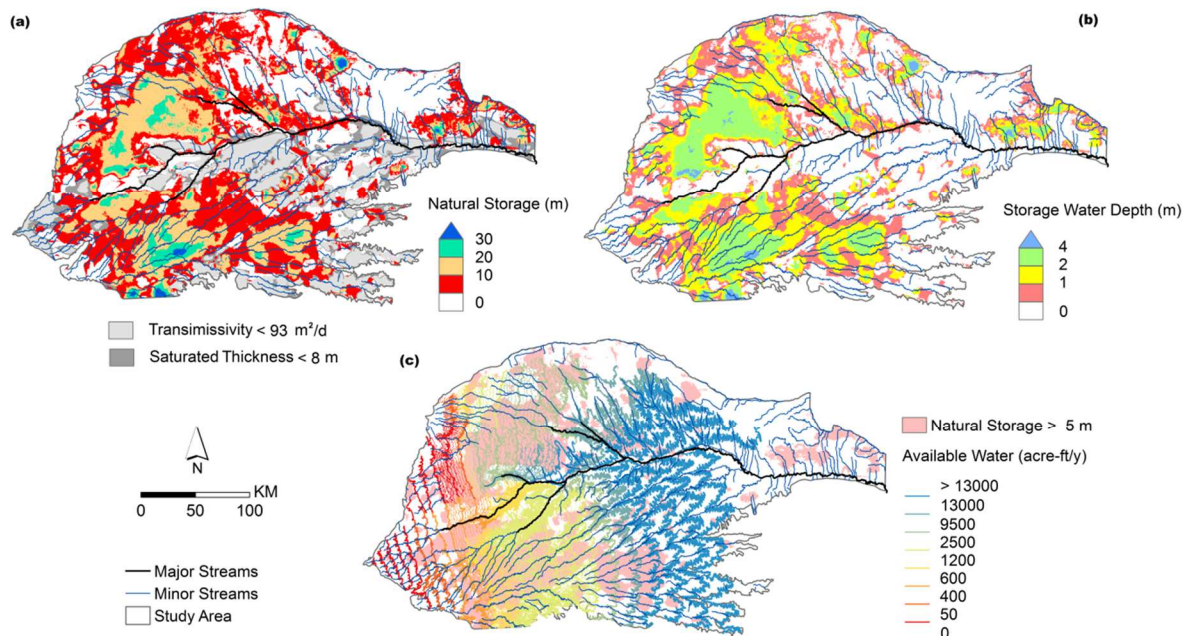


Figure 2.5: Potential ASR sites in the Republican River Basin can be identified by evaluating (a) natural storage thickness, (b) storage water depth, and (c) available water. *Storage water depth is defined as the product of natural storage and specific yield.*

Table 2.1 Average storage area in the Western portion of the Republican River Basin (km²).

| Available volume (Acre-ft/y) Average stored water depth (m) | | | | | | |
|---|------|------|------|------|------|-------|
| | 50 | 400 | 600 | 1200 | 2500 | 9500 |
| 1 | 0.06 | 0.49 | 0.74 | 1.48 | 3.08 | 11.72 |
| 2 | 0.03 | 0.25 | 0.37 | 0.74 | 1.54 | 5.86 |
| 3 | 0.02 | 0.16 | 0.25 | 0.49 | 1.03 | 3.91 |
| 4 | 0.02 | 0.12 | 0.19 | 0.37 | 0.77 | 2.93 |

We focused on the upstream portion of the Republican River to explore potential ASR sites, as this is the area where ASR is most likely to be cost effective. Large ASR natural storage areas are available in this region near losing rivers (Figure 2.6a). This region continues to have substantial declines in groundwater levels due to extensive pumping for irrigation. The points in Figure 3.6 labeled “Large ASR water source” are USGS gauges that could offer similar water volumes as the Equus Bed ASR project. The water table during predevelopment conditions would have been above the land surface in perennial stream reaches across the region. However there were few water levels available in the early development period to develop a water table map. Spreading basins combined with injection wells could likely be used to develop an ASR project of similar scale of the Equus Beds project. Alternatives include flooding irrigation fields during the dormant season and enhancing leakage from the current canal system or an expanded system (Figure 2.6b).

The two most upstream gauges (Figures 2.7, 2.8) frequently have significant peaks in flow from February to May during the dormant-season, thus available water could be diverted for ASR via off-season field irrigation. The other gauge (Figures 2.7c, 2.8c) has peak flows most

frequently during the growing season. But off-season peak flows that occur in later years despite pumping, could potentially be used for ASR. Storage area was calculated as available water divided by estimated storage water depth. For the western gauge, available water could be stored in a 5.7 km² area with 3m average water depth (Figure 2.6), while the central and eastern gauges provide estimates of available water of 24.8 km² and 57.5 km² respectively with 1 m average water depth.

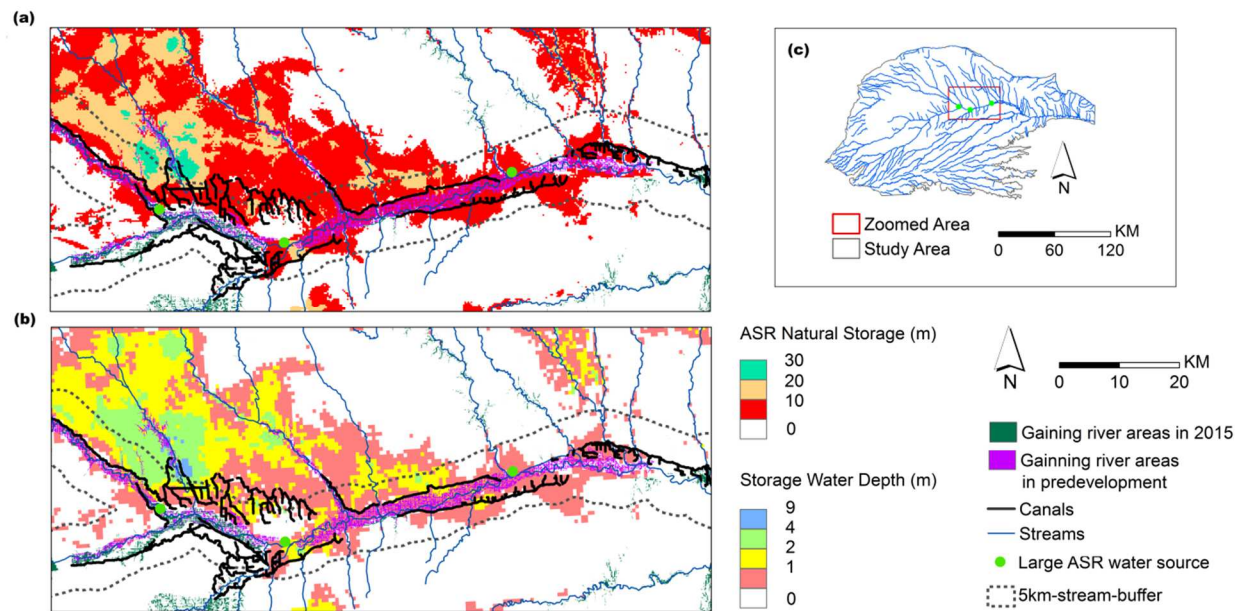


Figure 2.6: Map of potential ASR sites in the upper Republican River basin showing (a) natural storage thickness, (b) storage water depth, and (c) sites map. A 5 km-stream-buffer is shown between dashed lines as ASR is generally cost-effective with short transport distances. The points labeled “Large ASR water source” are USGS gauges that could offer similar water source as the Equus Bed ASR project. The predevelopment water table of most gaining river areas would have been near the land surface.

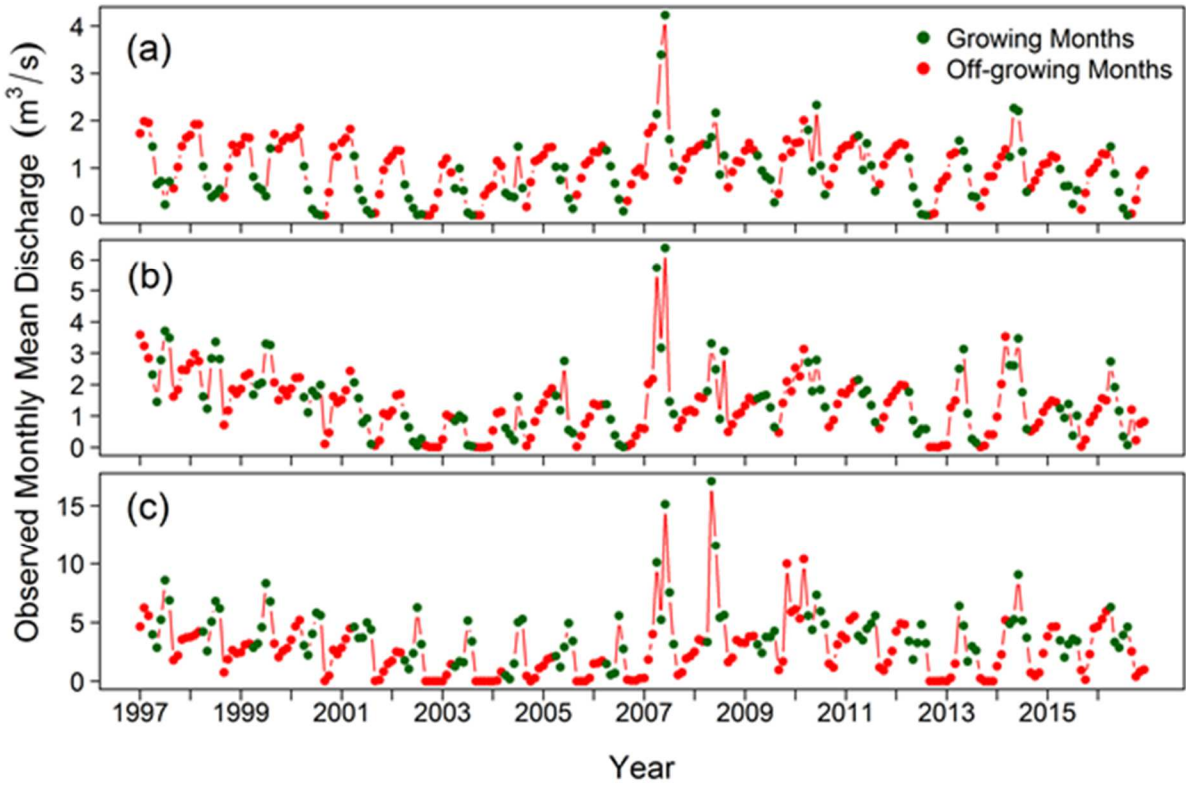


Figure 2.7: Observed mean monthly discharge at USGS gaging stations near potential ASR sites in the upstream portions of the Republican River basin. *Growing months were defined as May-August.* (a), (b), and (c) refer to three gauges with station numbers 06835500, 06837000, and 06843500. They are also labeled “Large ASR water source” (green solid circles) from left to right in Figure 2.6.

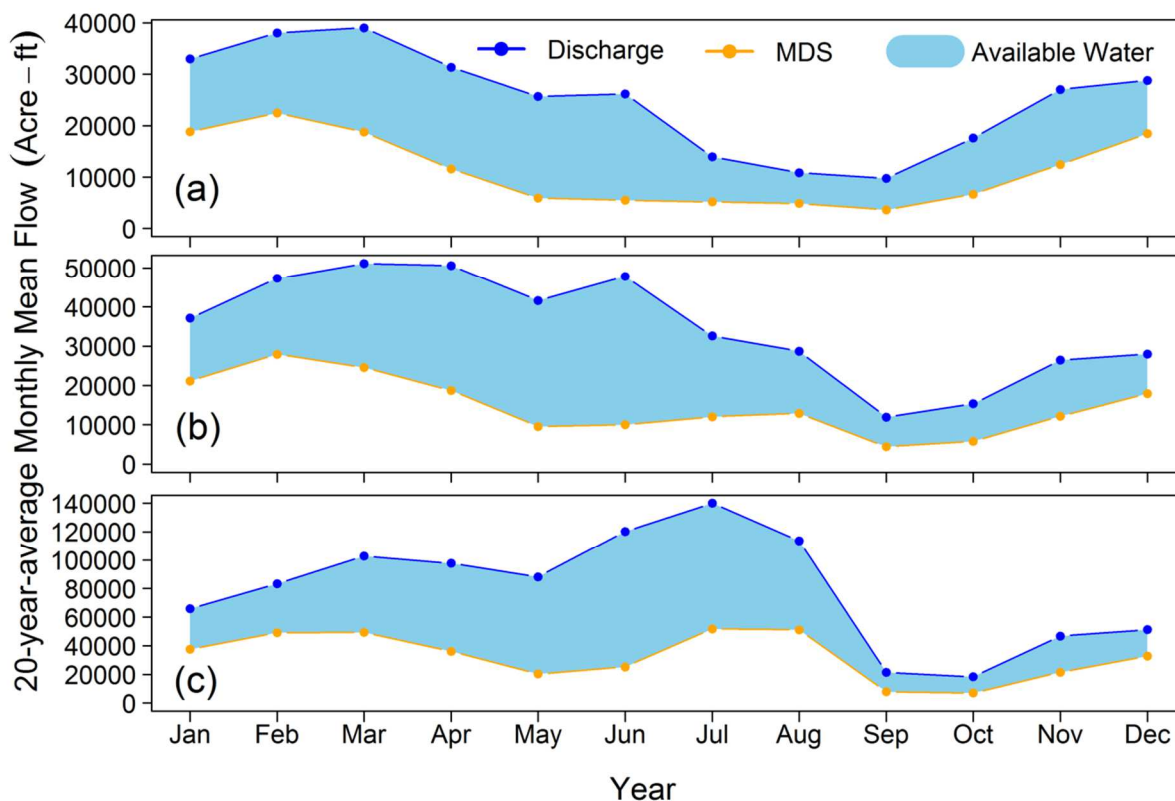


Figure 2.8: 20-year-average (1997-2016) monthly mean flow at USGS gaging stations near potential ASR sites in the upstream portions of the Republican River basin. *MDS* refers to the inferred Minimum Desirable Streamflow. (a), (b), and (c) refer to three gauges with station numbers 06835500, 06837000, and 06843500.

2.3 CONCLUSIONS

We develop a systematic method to estimate the potential viability of ASR for large regions. This includes the analysis of water source, conveyance, and recharge mechanisms. Water source analysis involves where and how much water is available; conveyance involves how water can be delivered to areas where it is needed; and recharge mechanisms reveal where impounded water can be efficiently stored and retrieved. Here, we evaluated the potential for ASR sites across the High Plains Aquifer, including natural storage thickness, and available water supply. For the Northern HPA, potential ASR sites are in the northeast and the Republican River Basin. Potential ASR sites

also exist in the central and eastern portions of the Central HPA, but there are few potential ASR sites in the Southern HPA due to the limitation of available water volume. Although ASR may be viable in a small number of flood events, we did not consider these in this study because such sites would not be economically viable.

This detailed analysis of the Republican River Basin indicates that there is likely available water across a large range of potential sites if water can be diverted from the Platte River to maintain required compact flows to Kansas. There are large natural storage volumes in the more arid western portion of the basin. Storage water depth and possible ASR volumes were also estimated. Extensive pumping of groundwater for irrigation in this basin has created a substantial volume of available storage and need for water. Our analysis indicates that one of the best potential sources of water is the Platte River, just to the North of the Republican River Basin. A water transfer from the North Platte River along the northwestern boundary of the study region could likely provide a substantial amount of water for ASR while maintaining flows into Kansas required by the compact agreement. Using current infrastructure, canal leakage and dormant season irrigation may provide a cost effective ASR mechanism in the upper Republican River basin.

REFERENCES

REFERENCES

- Ankit Saini. 2017. Artificial ground water recharge. LinkedIn SlideShare. Engineering, 26 Jan. 2015. Web. 07 Mar. 2017.
- Antoniou, E.A., P.J. Stuyfzand, B.M. van Breukelen. 2013. Reactive transport modeling of an aquifer storage and recovery (ASR) pilot to assess long-term water quality improvements and potential solutions. *Applied Geochemistry* 35 August: 173-186.
- Bakker M. 2010. Radial Dupuit interface flow to assess the aquifer storage and recovery potential of saltwater aquifers. *Hydrogeology Journal* 18:107–115.
<https://doi.org/10.1007/s10040-009-0508-1>
- Basagaoglu, H., and M.A. Marino. 1999. Joint management of surface and ground water supplies. *Ground Water* 37 (2): 214-222.
- Bloyd, R.M.. 1971. Underground storage of imported water in the San Geronio Pass area, southern California. U.S. Geological Survey Water-Supply Paper 1999- D, 37 p.
- Brown, Chris J. 2005. Planning decision framework for brackish water aquifer storage and recovery (ASR) projects, PhD dissertation: University of Florida. 414 p.
- Brown, Chris J., Weiss, Rebecca, Verrastro, Robert, Schubert, Steve. 2005. Development of an Aquifer, Storage and Recovery (ASR) site selection suitability index in support of the comprehensive Everglades restoration project. *Journal of Environmental Hydrology* 13(20):1-13.
- Carpenter, Tim. 2015. Missouri's Governor Throws Water on Kansas Aqueduct Idea. CJOnline.com. The Topeka Capital-Journal, 22 Jan. 2015. Web. 28 Oct. 2015.
- Deines, Jillian M., Anthony D. Kendall, and David W. Hyndman. 2017. “Annual Irrigation Dynamics in the U.S. Northern High Plains Derived from Landsat Satellite Data.” *Geophysical Research Letters* 44 (18): 9350–60. <https://doi.org/10.1002/2017GL074071>.
- Emmons, P.J. 1977. Artificial-recharge tests in upper Black Squirrel Creek Basin, Jimmy Camp Valley, and Fountain Valley, El Paso County, Colorado: U.S. Geological Survey Water-Resources Investigations Report 77-11, 49 p.
- Emmons, P.J. 1987. Preliminary assessment of potential well yields and the potential for artificial recharge of the Elm and Middle James Aquifers in the Aberdeen Area, South Dakota: U.S. Geological Survey Water Resources Investigation Report 87-4017, 33p.

- Environmental Protection Agency. 2016. Aquifer Recharge and Aquifer Storage and Recovery. EPA, Environmental Protection Agency, 29 Dec. 2016, www.epa.gov/uic/aquifer-recharge-and-aquifer-storage-and-recovery.
- Fleck , John. 2014. Aquifer to Benefit from Arroyo Project. Albuquerque Journal, 6 Nov. 2014, www.abqjournal.com/492057/aquifer-to-benefit-from-arroyo-project.html.
- Focazio, M.J., T.E. Reilly, M.G. Rupert, and D.R. Helsel. 2002. USGS Circular 1224, Assessing Ground-Water Vulnerability to Contamination: Providing Scientifically Defensible Information for Decision Makers, United States Geological Survey, Reston, Virginia, 28 p.
- Gillespie, J.B., and S.E. Slagle. 1972. Natural and artificial ground-water recharge, Wet Walnut Creek, central Kan-sas: Kansas Water Resources Board Bulletin no. 17, 94 p.
- Gillespie, J.B., G.D. Hargadine, and M.J. Stough. 1977. Artificial-recharge experiments near Lakin, western Kan-sas: Kansas Water Resources Board Bulletin no. 20, 91 p.
- Gutentag, D.E., J.F. Heimes, N.C. Krothe, Richard R. Luckey, and John B. Weeks. 1984. Geohydrology of the High Plains Aquifer in parts of Colorado, Kansas, Nebraska, New Mexico, Oklahoma, South Dakota, Texas, and Wyoming. USGS Professional Paper 1400-B
- Haacker, Erin M.K., Anthony D. Kendall, and David W. Hyndman. 2016. “Water Level Declines in the High Plains Aquifer: Predevelopment to Resource Senescence.” *Groundwater* 54 (2): 231–42. <https://doi.org/10.1111/gwat.12350>.
- Hamlin, S.N., 1987, Evaluation of the potential for artificial ground-water recharge in eastern San Joaquin County, California--Phase 3: U. S. Geological Survey Water-Resources Investigations Report 87-4164, 17 p.
- Händel, F., G. Liu, P. Dietrich, R. Liedl, J. Butler. 2014. Numerical assessment of ASR recharge using small-diameter wells and surface basins. *Journal of Hydrology* 517: 54-63. <https://doi.org/10.1016/j.jhydrol.2014.05.003>.
- Harvey, F.E., S.S. Sibray. 2001. Delineating ground water recharge from leaking irrigation canals using water chemistry and isotopes. *Groundwater* 39 (3):408-421.
- Hernandez, E. A., Venkatesh Uddameri, Marcelo A. Arreola Jr. 2014. A multi-period optimization model for conjunctive surface water–ground water use via aquifer storage and recovery in Corpus Christi, Texas. *Environmental Earth Sciences* 71 (6): 2589-2604.
- Houston, N.A., Gonzales-Bradford, S.L., Flynn, A.T., Qi, S.L., Peterson, S.M., Stanton, J.S., Ryter, D.W., Sohl, T.L., and Senay, G.B., 2013, Geodatabase compilation of hydrogeologic, remote sensing, and water-budget-component data for the High Plains aquifer, 2011: U.S. Geological Survey Data Series 777, 12 p., <http://pubs.usgs.gov/ds/777/>.

- IWMI-Tata Water Policy Program. 2002. Innovations in Groundwater Recharge. Water Policy Briefing, Issue1
- Jackson, Kyle. 2009. A Survey of Western United States Instream Flow Programs and The Policies that Protect a River's Ecosystem. Environmental Studies Undergraduate Student Theses. 28.
- Kansas Water Appropriation Act. 1984. 82a-703a, b and c
- Koch, N.C. 1984. Effects of artificial recharge on the Big Sioux Aquifer in Minnehaha County, South Dakota. U.S. Geological Survey Water-Resources Investigations Report 84-4312, 8 p.
- Lichtler, W.F., D.I. Stannard, and E. Kouma. 1980. Investigation of artificial recharge of aquifers in Nebraska: U.S. Geological Survey Water-Resources Investigations Report 80-93, 112 p.
- Lowry, C. S., M.P. Anderson. 2006. An Assessment of Aquifer Storage Recovery Using Ground Water Flow Models. *Groundwater* 44(5): 661–667.
- McGuire, V.L. 2012. Water-level and storage changes in the High Plains Aquifer, predevelopment to 2011 and 2009–11. USGS Scientific Investigations Report 2012-5291. Reston, Virginia: USGS.
- Mosch, M.J.M. 1998. Dynamic simulation model for water management of a large-scale artificial recharge system: in Peters, Jos H. ed., Artificial recharge of ground water, Proceedings of the Third International Symposium, Amsterdam, Netherlands, 1998: A.A. Balkema, Rotterdam, Netherlands and Brookfield, VT, p. 15-20.
- Niswonger, R. G., E. D. Morway, E. Triana, and J. L. Huntington. 2017. Managed aquifer recharge through off-season irrigation in agricultural regions. *Water Resour. Res.* 53. <https://doi.org/10.1002/2017WR020458>
- Philbrick, C. R., and P. K. Kitanidis. 1998. Optimal conjunctive-use operations and plans. *Water Resources Research* 34(5): 1307-1316.
- Phillips, S. P. 2002. The Role of Saturated Flow in Artificial Recharge Projects. U. S. Geological Survey Artificial Recharge Workshop Proceedings, Sacramento, California, April 2-4, 2002. U. S. Geological Survey Open-File Report 02-89, p. 17-20.
- Prill, R. C., 1977. Movement of moisture in the unsaturated zone in a loess-mantled area, southwestern Kansas. U.S. Geological Survey Professional Paper 1021, 21 p.
- RRCA (Republican River Compact Administration), 2003, Groundwater model documentation. Online at <http://www.republicanrivercompact.org>.

- Signor, D.C., D.J. Growitz, and William Kam. 1970. Annotated bibliography on artificial recharge of ground water. U.S. Geological Survey Water-Supply Paper 1990, p.1.
- Sumner, D.M., W.M. Schuh, and R.L. Cline. 1991. Field experiments and simulations of infiltration-rate response to changes in hydrologic conditions for an artificial-recharge test basin near Oakes, southeastern North Dakota. U.S. Geological Survey Water-Resources Investigations Report 91-4127, 46 p.
- Taylor, O.J. 1975. Artificial-recharge experiments in the alluvial aquifer south of Fountain, El Paso County, Colorado: Colorado Water Resources Circular no. 31, 28 p.
- Thandaveswara, B.S., 2017. Hydraulics lecture. Indian Institute of Technology Madras.
- Todd, D.K. 1959. Annotated bibliography on artificial recharge of ground water through 1954: U.S. Geological Survey Water-Supply Paper 1477, 115 p.
- U.S. Army Corps of Engineers. 2015. Aquifer Storage and Recovery (ASR) Regional Study. U.S. Army Corps of Engineers, Apr. 2015, www.saj.usace.army.mil/Missions/Environmental/Ecosystem-Restoration/Aquifer-Storage-and-Recovery-ASR-Regional-Study/.
- U.S. National Research Council. 1994. Ground water recharge using waters of impaired quality. National Academy Press, 1994. <https://books.google.com/books?id=5QtSAAAAMAAJ>
- Vanderzalm, J.L., D.W. Page, K. E. Barry, P. J. Dillon. 2013. Application of a probabilistic modelling approach for evaluation of nitrogen, phosphorus and organic carbon removal efficiency during four successive cycles of aquifer storage and recovery (ASR) in an anoxic carbonate aquifer. *Water Research* 47(7): 2177-2189.
- Ward J.D., C.T. Simmons, P.J. Dillon, P. Pavelic. 2009. Integrated assessment of lateral flow, density effects and dispersion in aquifer storage and recovery. *Journal of Hydrology* 370:83–99.
- Weeks, E.P. 2002. A Historical Overview of Hydrologic Studies of Artificial Recharge in the U.S. Geological Survey. U. S. Geological Survey Artificial Recharge Workshop Proceedings, Sacramento, California, April 2-4: U. S. Geological Survey Open-File Report 02-89, p. 17-20.
- Ziegler, A.C., C.V. Hansen, and D.A. Finn. 2010. Water Quality in the Equus Beds Aquifer and the Little Arkansas River Before Implementation of Large-Scale Artificial Recharge, South-Central Kansas, 1995–2005: U.S. Geological Survey Scientific Investigations Report 2010–5023, 143 p.
- Zuurbier, K. G. Bakker, M., Zaadnoordijk, W. J. Stuyfzand, P. J. 2013. Identification of potential

sites for aquifer storage and recovery (ASR) in coastal areas using ASR performance estimation methods. *Hydrogeology Journal* 21 (6): 1373-1383.
<https://doi.org/10.1007/s10040-013-1003-2>